



**UNIVERSIDAD DE INVESTIGACIÓN DE
TECNOLOGÍA EXPERIMENTAL
YACHAY**

Escuela de Ciencias Físicas y Nanotecnología

**TÍTULO: On the Page curve for a Taub-Nut black
hole**

Trabajo de integración curricular presentado como
requisito para la obtención
del título de Físico

Autor:

Vicente Alexander Arévalo Nazate

Tutor:

Ph.D Clara Rojas

Co - Tutor:

M.Sc David Andrade

Urcuquí, Mayo 2024

AUTORÍA

Yo, **Vicente Alexander Arévalo Nazate**, con cédula de identidad 0401993605, declaro que las ideas, juicios, valoraciones, interpretaciones, consultas bibliográficas, definiciones y conceptualizaciones expuestas en el presente trabajo; así como, los procedimientos y herramientas utilizadas en la investigación, son de absoluta responsabilidad de el/la autora (a) del trabajo de integración curricular. Así mismo, me acojo a los reglamentos internos de la Universidad de Investigación de Tecnología Experimental Yachay.

Urququí, Mayo 2024.

Vicente Alexander Arévalo Nazate
CI: 0401993605

AUTORIZACIÓN DE PUBLICACIÓN

Yo, **Vicente Alexander Arévalo Nazate**, con cédula de identidad 0401993605, cedo a la Universidad de Investigación de Tecnología Experimental Yachay, los derechos de publicación de la presente obra, sin que deba haber un reconocimiento económico por este concepto. Declaro además que el texto del presente trabajo de titulación no podrá ser cedido a ninguna empresa editorial para su publicación u otros fines, sin contar previamente con la autorización escrita de la Universidad.

Asimismo, autorizo a la Universidad que realice la digitalización y publicación de este trabajo de integración curricular en el repositorio virtual, de conformidad a lo dispuesto en el Art. 144 de la Ley Orgánica de Educación Superior

Urququí, Mayo 2024.

Vicente Alexander Arévalo Nazate
CI: 0401993605

Dedication

This project is dedicated to my entire family. Especially to my loving parents, Vicente and Fanny, who have always taught me that to achieve the goals that arise in life, you have to be patient and disciplined, for their unwavering support, sacrifice, and boundless love. To my twin sisters Ivone and Marisol and my sister Valeria, thank you for your unconditional friendship and always believing in me. To the memory of my grandmother Carmen, I know she would be proud to see where I have come.

This thesis is for all of you...

Vicente Alexander Arévalo Nazate

Acknowledgements

In particular, I would like to thank my family for their unconditional support during my academic trajectory. I express my deep gratitude to my aunt Alba, Javier and their corresponding families, for always offering me the opportunity to have another family during these years.

I desire my especial gratitude to my advisors Clara and David for bringing me the opportunity to work with them. Thanks for their guidance, support, and encouragement throughout my research project.

I want to thank professors Wladimir, Helga, Duncan, Patricio, Franklin, Gema, and Henry, who constantly support my passion for science and have practically shaped me into a good professional.

To my friends Daniel, Brandon, Osmer, Franklin; thanks for the laughs, for making physics more fun. To Roy, Saire, Santiago, and Diego who always encouraged me to keep going and not give up.

Finally, I would like to thank everyone who supported me during all these years, without their support all this would not have been possible.

Vicente Alexander Arévalo Nazate

Resumen

En 1975, Stephen Hawking, en su artículo "Particle Creation by Black Holes," propuso que se generan pares de partículas virtuales debido a efectos de la mecánica cuántica cerca del horizonte de sucesos de un agujero negro. Una de estas partículas escapa al infinito en forma de radiación de Hawking. Como resultado, se ha teorizado que los agujeros negros no son completamente "negros". Además, debido a la radiación de Hawking, los agujeros negros y su información tienden a desaparecer, lo que lleva a la paradoja de la pérdida de información. En 1993, Page propuso una posible solución a esta paradoja. Él hizo uso de la entropía de Von Neumann para cuantificar nuestro conocimiento sobre la información de los agujeros negros, asumiendo que un agujero negro y su radiación son un estado cuántico puro. Esta entropía, cuya evolución temporal se conoce como curva de Page, debe tender a cero cuando el proceso de "evaporación" tiende a finalizar, implicando recuperación de información. La curva de Page ha sido ampliamente estudiada para diferentes modelos de agujeros negros, incluidos los agujeros negros de Kerr y Schwarzschild. En ese sentido, en el presente trabajo estudiamos la radiación de Hawking para un agujero negro de Kerr-Taub-Nut descrito por su masa, momento angular y parámetro de nut a través de la emisión de partículas escalares sin masa (e.g., bosones). Mostramos que el momento angular se pierde más rápido que el parámetro de nut y la masa en el proceso de evaporación del agujero negro. Del mismo modo, utilizando el modelo de evolución de los parámetros de un agujero negro propuesto por Page, estudiamos la evolución de la entropía de Von Neumann para la radiación de Hawking, proporcionando así una descripción de la curva de Page para un agujero negro de Kerr-Taub-Nut.

Palabras clave: Agujero negro de Kerr-Taub-Nut , Radiación de Hawking , Curva de Page.

Abstract

In 1975, Stephen Hawking, in his paper "Particle Creation by Black Holes," proposed that pairs of virtual particles are generated due to quantum mechanical effects near the event horizon of a black hole. One of these particles escapes to infinity in the form of Hawking radiation. As a result, it has been theorized that black holes are not entirely "black." Moreover, due to Hawking radiation, black holes and their information tend to disappear, leading to the Information Loss Paradox. In 1993, Page proposed one possible solution to this paradox. He used the Von Neumann entropy to quantify our knowledge about black hole information, assuming that a black hole and its radiation are a pure quantum state. This entropy, whose temporal evolution is known as the Page curve, must tend to zero when the "evaporation" process tends to end, implying information recovery. The Page curve has been extensively studied for different black hole models, including Kerr and Schwarzschild black holes. In that sense, in the present work, we study the Hawking radiation for a Kerr-Taub-Nut black hole described by its mass, angular momentum, and nut parameter through the emission of massless scalar particles (e.g., bosons). We show that angular momentum is lost faster than nut charge and mass in the black hole evaporation process. In the same way, using the model for the evolution of the parameters of a black hole proposed by Page, we studied the evolution of the Von Neumann entropy for Hawking radiation thereby providing a description of the Page curve for a Kerr-Taub-Nut black hole.

Keywords: Kerr-Taub-Nut black hole, Hawking radiation, Page Curve.

Contents

List of Figures	xvi
List of Tables	xviii
1 Introduction	1
1.1 Problem Statement	2
1.2 General and Specific Objectives	2
2 Methodology	5
2.1 Taub-Nut Space-Time	5
2.1.1 Kerr-Taub-Nut Black Hole	7
2.2 Dynamics of a Minimally Coupled Massless Scalar Field	10
2.2.1 Effective Potential	10
2.3 Hawking Radiation	12
2.3.1 Entropy and Thermodynamics	12
2.3.2 Greybody Factors	14
2.3.3 Emission Rates	15
2.3.4 Black hole evaporation and Information Loss Paradox	16
2.4 The Page Curve	18
2.4.1 The Fine-Grained Entropy	18
2.4.2 Correlation between the Black Hole and its Radiation	19
2.4.3 The Time Dependence of the Von Neumann Entropy	20
3 Results & Discussion	23
3.1 Thermodynamics for a Kerr-Taub-Nut Black Hole	23
3.1.1 Temperature	23
3.1.2 Bekenstein-Hawking Entropy	26
3.2 Massless Scalar Field in Kerr-Taub-Nut Space-Time	27
3.2.1 Effective Potential	28

3.2.2	Effective potential at the horizon	30
3.3	Hawking Radiation for a KTN Black Hole	31
3.3.1	Gray Body Factor	31
3.3.2	Emission Rates	34
3.4	Differential decays.	38
3.5	The Page Curve for a Kerr-Taub-Nut Black Hole	39
3.5.1	Time dependence of the Kerr-Taub-Nut black hole	39
3.5.2	The Von Neumann Entropy	43
4	Conclusions and outlook	49
A	Taub-Nut space-time	51
B	Derivation of the Bekenstein-Hawking entropy	53
C	Modeling the Time Evolution for the Kerr-Taub-Nut Black Hole Parameters	55
D	Mathematica code to calculate the entropy of Hawking radiation	57
	Bibliography	59

List of Figures

2.1	Schematic representation of a TN space-time.	7
2.2	Schematic representation of the cross section for a Kerr-Taub-Nut black hole.	8
2.3	Effective potential mechanism sketch	11
2.4	Hawking radiation sketch	12
2.5	Grey-body radiation from a black hole.	15
2.6	Stages of black hole evaporation	16
2.7	Quantum representation of a black hole.	17
2.8	Entropies involved in the process of black hole evaporation	20
3.1	Temperature dependence of mass for a Kerr-Taub-Nut black hole	24
3.2	Temperature dependence on the rotation parameter for a Kerr-Taub-Nut black hole	25
3.3	Plots of V_{eff} (3.14) for various values of the nut parameter l and rotation parameter a . Here the parameters are $M = 4$, $\omega = 10$, $\ell = m = 1$ (l and a are in solar masses).	29
3.4	Plots of the effective potential at the event horizon $V_{horizon}$ given by expression (3.16) for various values of the rotation parameter a (in solar masses). Here, we set $m = 1$, $l = 0.25 M_{\odot}$	31
3.5	Plots of the grey-body factors $\gamma_{\ell 0}(\omega)$ (3.14) for various situations. (a) $M = 1$, $a = 0.5$, $l = 0.3$, (b) $\ell = 1$, $a = 0.5$, $l = 0.3$, (c) $M = 1$, $\ell = 1$, $l = 0.3$, (d) $M = 1$, $\ell = 1$, $a = 0.5$ (M , a , l are in solar masses)	33
3.6	Energy emission rate for KTN black hole for different masses M . We set the parameters $a = 0.7$, $l = 0.3$	36
3.7	Angular momentum emission rate for KTN black hole for different rotation parameters a . We set the parameters $M = 2$, $l = 0.3$	37
3.8	Nut parameter emission rate for KTN black hole for different nut parameters l . We set the parameters $M = 2$, $a = 0.7$, and $n = 0.15$	38
3.9	Mass-time dependence profiles for different black hole masses.	41
3.10	Angular momentum-time dependence profiles for different black hole initial angular momentum. The physical parameters are $M = 3 M_{\odot}$ and $l = 0.3 M_{\odot}$	42
3.11	Nut parameter time dependence profiles for different initial nut values. The parameters are $M = 3 M_{\odot}$ and $a = 0.4 M_{\odot}$	43

3.12	Bekenstein-Hawking entropy evolution $S_{BH}(t)$ for a Kerr-Taub-Nut black hole. The physical parameters are: $M(0) = 2, J(0) = 0.6, l(0) = 0.2$	44
3.13	Entropy of Hawking radiation evolution $S_{BH}(t)$ for a Kerr-Taub-Nut black hole. The Physical parameters are: $M(0) = 2, J(0) = 0.6, l(0) = 0.2$	45
3.14	Von Neumann entropy evolution for an initially pure KTN black hole. $M = 2, J = 0.6, L = 0.2$ (thick line), $M = 3.0, J = 1.2, l = 0.30$ (dashed line).	46
3.15	Von Neumann entropy evolution for an initially pure KTN black hole for different β values. We set $M = 2, J = 0.6, l = 0.2$	47

List of Tables

2.1	Summary of the entropies presented in the thesis.	21
3.1	Bekenstein-Hawking entropy for a Kerr-Taub-Nut, Kerr, and Schwarzschild black holes.	26
3.2	Differential decays for the mass, angular momentum and nut parameter. The fundamental nut parameter is defined as $n = 0.15$	39
3.3	Lifetime for different KTN black hole masses.	41
3.4	Page time for an initially pure KTN black hole for different β values. $M = 2 M_{\odot}$, $J = 0.6 M_{\odot}^2$, $l = 0.2 M_{\odot}$	47

Chapter 1

Introduction

It is well-known that black holes (BHs) are characterized by the fact that light and matter can enter but never go out. Typically, there are regions where gravity is so strong that even light cannot escape, which makes these regions black objects in space¹. However, in 1975, Hawking found that BHs are not totally black. This happens due to quantum fluctuations that lead to particle creation near the event horizon. Thus, BHs can emit particles as Hawking radiation.

In this context, Hawking radiation represents a revolutionary topic as a consequence of the fact that general relativity and quantum mechanics can work together in order to explain our Universe. Additionally, Hawking radiation has several implications in theoretical physics². For example, Hawking radiation implies that BHs must be treated as thermal systems with temperature and entropy.

Nonetheless, due to Hawking radiation, BHs tend to evaporate after a long period. In this case, however what happens with the information stored in the matter swollen by the black hole? At first glance, it could be possible to say that information is lost forever. From another point of view, such information could be conserved as a consequence of some mechanism allowing it to be encoded in Hawking radiation.

The central question of the information paradox is whether the process of formation and evaporation of a black hole can be described in a unitary fashion. For this reason, it is essential to consider the Von Neumann entropy. This entropy is a measure of the incomprehension of a quantum state¹. In particular, unitarity implies that the Von Neumann entropy of the Hawking radiation (i.e., it is possible to consider radiation as a quantum state) should initially rise but then fall back down³. In 1993, Page in the paper *Information in Black Hole radiation*⁴ proposed that information is conserved as a consequence of quantum mechanical considerations that implies that information can come out very slowly and that the result is not a very chaotic system like a disordered gas⁵. He generally considered the black hole and its radiation can be treated as a single quantum state. In other words, Page plotted the time evolution of the Von Neumann entropy under semiclassical considerations correlating the black hole entropy and its radiation. This plot is known as the "Page curve," which implies that if the entropy follows this profile, the information is preserved in the black hole evaporation process.

The Page curve guarantees that information is conserved. The mechanism behind this process still needs to be identified. However, in the search for this process, new horizons in theoretical physics have been identified, for

example, the holographic principle and some theories related to quantum gravity³. Furthermore, in the context of these new theories, methods like the Ryu-Takayanagi formula⁶, minimal quantum extremal surface^{3,7}, and the island method⁸⁻¹⁰, have been developed in order to calculate the "Page curve," so that the Page curve represents an active topic in theoretical physics.

1.1 Problem Statement

In general relativity, Einstein's field equations have several solutions describing different space times. One of the most common metrics is the Schwarzschild metric, which describes the space-time around a massive, spherically symmetric object (its mass describes the metric). In the same way, the Kerr metric describes the space-time around a rotating object (the mass and angular momentum describe it). Additionally, the metrics could contain a nut parameter, giving origin to Taub-Nut (Newman, Unti, Tamburino) space-time. The physical interpretation of the nut parameter still needs to be better defined, but in some situations, it could be regarded as a magnetic monopole, which is only possible in theory, and also, the nut parameter could be considered a source of angular momentum. Moreover, metrics containing nut parameters work very well in theoretical physics to explain some aspects of string theory and the construction of quantum gravity theories¹¹.

When we combine the mass, angular momentum, and the nut parameter, it is possible to get the Kerr-Taub-Nut metric. Generally, the metric describes the space-time around a rotating object with mass and nut parameter l . The KTN metric can describe a black hole, and in the last few dates, it has aroused much interest in the scientific community. For example, it has been theoretically examined the existence of the nut parameter in M87* and Sgr A* by numerically deducing the shadow sizes in Kerr-Taub-Nut (KTN) space-time based on the data provided by the Event Horizon Telescope image¹²⁻¹⁴. In the same way, the KTN space-time was used to explain the jet power and the radiative efficiency of black holes in different X -ray binary systems¹⁵. The authors used the Novikov-Thorne model, which assumes that the disc is geometrically thin, so particles move very close to the equatorial plane. Moreover, they consider the effective potential generated by the metric in order to include the parameters that describe the itself. Consequently, this work aims to study the Hawking radiation for a Kerr-Taub-Nut black hole in order to describe the "Page Curve," based on the work of Page¹⁶ and Nian¹⁷.

1.2 General and Specific Objectives

This project aims to calculate the Hawking radiation for a Kerr-Taub-Nut black hole, considering that the field that is surrounding the black hole is a massless scalar field in order to give a description of the Page curve for a Kerr-Taub-Nut black hole. In pursuit of the objective, the following tasks are specified:

- To briefly describe the thermodynamics for a KTN black hole, including an analysis of the temperature and the Bekenstein-Hawking entropy.
- To study the dynamics of a massless scalar field in the presence of a KTN black hole, where the most critical aspect is describing the black hole's effective potential.

- To calculate and analyze the greybody factors, which quantify the deviation of the Hawking radiation from pure blackbody radiation, for a KTN black hole.
- To calculate the Hawking radiation for a KTN black hole. It is important to mention that previous steps are needed to get the specified radiation.
- To analyze the rates at which the black hole parameters change during evaporation.
- To calculate the time evolution of the parameters that describe the black hole.
- To calculate and describe the time evolution of the Bekenstein-Hawking entropy and the radiation entropy.

The organization of the thesis is as follows. In chapter 2, a brief description of the space-times containing a nut parameter is given, specifically the KTN space-time. After that, theoretical aspects behind the Page curve calculation are presented. Firstly, the dynamics of a black hole in a massless scalar field is described to understand the origin of the Hawking radiation. Once the Hawking radiation is explained, a short thermodynamical analysis is given, including the temperature and entropy in the context of black holes. Finally, the method to obtain the evolution of the black hole parameters, which are essential to get the Page curve, is discussed. In chapter 3, all the theoretical aspects described in the previous chapter are applied and discussed in the context of a Kerr-Taub-Nut black hole. Finally, the conclusions and future work are shown in chapter 4.

Throughout the work, the spacelike signature for the KTN space-time will be considered as $(-, +, +, +)$, and natural units will be used (until otherwise specified) to simplify the notation such that

$$\hbar = c = G = K_B = 1,$$

where K_B is the Boltzmann's constant.

Chapter 2

Methodology

This chapter delves into the theoretical framework on which the research is based. We start by briefly describing the space-time involving the nut parameter. Then, we present a description of the Hawking radiation, together with a short thermodynamics analysis. Finally, a brief summary explains how the Page curve could be considered a solution for the information paradox.

2.1 Taub-Nut Space-Time

In 1951, Taub discovered a new spatially homogeneous empty space solution of Einsteins' equations¹⁸. This solution could be interpreted as a vacuum homogeneous cosmological model¹⁹. After that, in 1963, Newman, Tamburino, and Unti rediscovered the metric²⁰. In that case, the metric was considered a generalization of the Schwarzschild space-time. The main characteristic of the metric is that it contains the so called nut parameter (interpretations will given below). This metric has played an important role into the eventual discovery of the well-known rotating Kerr black hole solution. For this reason, the Tab-Nut metric is considered as the first attend to have a space-time generated by a rotating object^{20,21}.

Nevertheless, TN space-time could be considered a line of investigation to look for anomalies or unique characteristics of different space-times (e.g., Kerr, Kerr-Newmann, etc. All of them, containing the nut parameter)²². Moreover, this solution is now being reconsidered in the context of higher-dimensional theories of semi-classical quantum gravity²³. Additionally, it is essential to describe the nature of some aspects within the String theory framework and its relation with the M-theory¹¹. Therefore, the TN metric is a valuable guide in unveiling new aspects of theoretical physics.

The NUT solution is often quoted in the form

$$ds^2 = -f(r)(d\bar{t} - 2l \cos \theta d\phi)^2 + \frac{dr^2}{f(r)} + (r^2 + l^2)(d\theta^2 + \sin^2 \theta d\phi^2), \quad (2.1)$$

where

$$f(r) = \frac{r^2 - 2Mr - l^2}{r^2 + l^2}, \quad (2.2)$$

and M and l are the mass and nut parameter, respectively.

The line element (2.1) reduces to the Schwarzschild space-time when $l \rightarrow 0$. The Taub-Nut (TN) space-time has different interpretations. One of the interpretations for the TN metric is that it describes a space-time with a black hole of mass M , nut parameter l , and its corresponding event horizon. Because of the $l \cos \theta$ term in the metric (2.1), the space-time does not have a well-behaved axis at both $\theta = 0$ and $\theta = \pi$ ²³. It happens because at this values the term $l \cos \theta$ change from $-l$ to l . This behaviour is regarded to the present of cosmic strings or a line singularity at the poles. In general, the presence of the nut parameter l allows to the TN space-time has a singular line, part of which is surrounded by closed timelike curves^{21,23-25}(see appendix A for more details).

As we mentioned before, the nut parameter l is the main feature of the TN metric, but ¿what is the physical interpretation of this parameter? First, to answer the question, let us consider the cosmic strings that we discussed in the previous paragraph. Bonnor²⁶ physically considered strings as a semi-infinite massless source of angular momentum²³. Moreover, it is considered a twist (i.e., rotation) source that injects angular momentum into the space-time. Therefore, the nut parameter quantifies the amount of angular momentum of the source.

From an electromagnetic point of view, the nut parameter gives space-time a gravitomagnetic monopole interpretation^{27,28}. The theoretical evidence is that when light rays pass through the origin, they are not bent. Instead, they suffer twisting effects, which produce a spiral shear in the path of the rays, an effect that Dirac monopoles should produce. So, the nut parameter l describes the strength of the gravitomagnetic monopole, which is the gravitational analog of the magnetic monopole in Maxwell's electrodynamics. Furthermore, considering the Dirac theory, if the monopoles exist, they must be connected to a Dirac string. Therefore, the cosmic strings could be considered the analog of the Dirac case²³ (see figure 2.1). Additionally, it is essential to mention that the strings do not affect the space-time.

Additionally, the space-time associated with the TN metric is locally asymptotically flat but not globally asymptotically flat. Nevertheless, neglecting the effect of the parameter at infinity, it could be considered an asymptotically flat space. Finally, as a consequence, there has yet to be a consensus about the general description of the nut parameter. However, in this work, we will adapt Bonnor's²⁶ interpretation of the metric, which implies that the metric contains a massless source of angular momentum. Therefore, the nut parameter l will be regarded as a quantity that describes this angular momentum.

Additionally, it is essential to mention that in 1976, Plebánski and Demiański²⁹ presented a general metric that contains all the metrics associated with a gravitational field of isolated massive objects. The nice part of this metric is that it contains all the parameters that characterize the different space-times. For example, the charge, mass, angular momentum, cosmological constant, and nut parameter, among others. Therefore, with this canonical metric and the correct combination of the parameters, it is possible to describe the most common space-times, such as Schwarzschild, Kerr, Kerr-Newmann, Taub-Nut, among others.

Practically, TN space-time lies entirely in the theoretical frame because there is no evidence of its existence. Despite this, using the Plebánski and Demiański metric, it is possible to have different space-times. One exciting situation happens when a combination of the mass, angular momentum, and the nut parameter raises the possibility

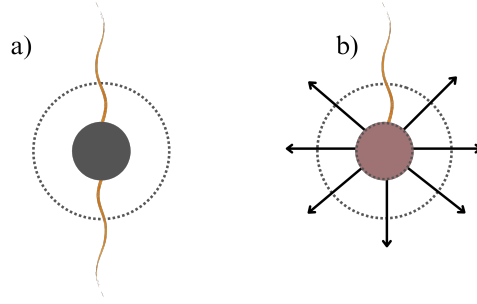


Figure 2.1: a) Schematic representation of a Taub-Nut space-time with the corresponding cosmic strings at the poles. b) The hypothetical magnetic monopole with its corresponding Dirac string at the north pole. For this reason, TN space-time is regarded as the gravitomagnetic analog of the magnetic monopole.

of having a Kerr-Taub-Nut (KTN) space-time²⁴, which is the purpose of this work, and its importance relies on the possibility to have theoretical evidence of its existence as we discussed in section 1.1.

2.1.1 Kerr-Taub-Nut Black Hole

As discussed, if the Kerr space-time contains the nut parameter, it is regarded as the Kerr-Taub-Nut space-time, which is also an analytic solution to the vacuum Einstein equations. Generally, it represents the gravitational field of a rotating body with mass and nut parameter l . Here we give the explicit form of the Kerr-Taub-Nut metric in Boyer-Lindquist coordinates (t, r, θ, φ) which is described by the following line element^{30–35}:

$$ds^2 = -\frac{1}{\Sigma} (\Delta - a^2 \sin^2 \theta) dt^2 + \frac{2}{\Sigma} [\Delta \chi - a(\Sigma + a\chi) \sin^2 \theta] dt d\varphi + \frac{1}{\Sigma} [(\Sigma + a\chi)^2 \sin^2 \theta - \chi^2 \Delta] d\varphi^2 + \frac{\Sigma}{\Delta} dr^2 + \Sigma d\theta^2, \quad (2.3)$$

where parameters Σ , Δ , and χ are given by the following expressions:

$$\Delta(r) = r^2 - 2Mr - l^2 + a^2, \quad (2.4)$$

$$\Sigma(r, \theta) = r^2 + (l + a \cos \theta)^2, \quad (2.5)$$

$$\chi(\theta) = a \sin^2 \theta - 2l \cos \theta, \quad (2.6)$$

and M , a , l are the mass, rotation parameter, and nut parameter, respectively, and $r \in [0, +\infty]$, $t \in [0, +\infty]$, $\theta \in [0, \pi]$, and $\varphi \in [0, 2\pi]$. Moreover, the angular momentum is defined as $J = aM$. From the line element it is possible to identify the same properties of the space-time³⁶.

1. It is axisymmetric, since it does not depend on the azimuthal angle φ .
2. It is stationary, since it does not depend on time.
3. Imposing the flatness condition, the space-time at infinity could be treated as Minkowsky space-time³³.

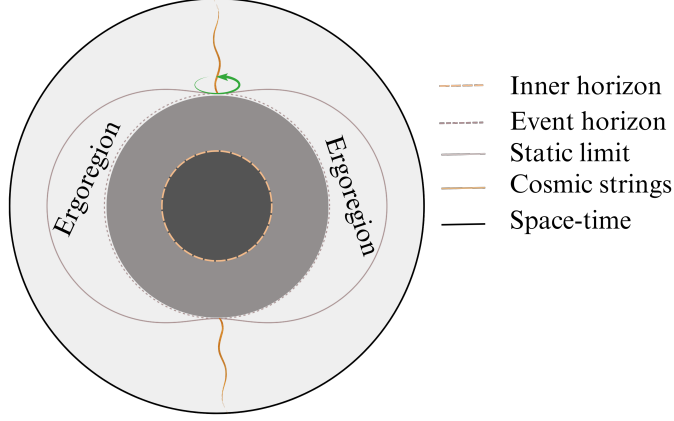


Figure 2.2: Schematic representation of the cross section for a Kerr-Taub-Nut black hole.

As the KTN space-time is a family of the Kerr metrics, it could be possible to have the same properties as Kerr³⁷. The metric in matricial form is given by:

$$g_{\mu\nu} = \begin{pmatrix} g_{tt} & 0 & 0 & g_{t\varphi} \\ 0 & \frac{\Sigma}{\Delta} & 0 & 0 \\ 0 & 0 & \Sigma & 0 \\ g_{t\varphi} & 0 & 0 & g_{\varphi\varphi} \end{pmatrix}, \quad (2.7)$$

where the metric elements are the same as the line element (2.3), which are denoted by:

$$g_{tt} = -\frac{1}{\Sigma} (\Delta - a^2 \sin^2 \theta), \quad (2.8)$$

$$g_{rr} = \frac{\Sigma}{\Delta}, \quad (2.9)$$

$$g_{\theta\theta} = \Sigma, \quad (2.10)$$

$$g_{t\varphi} = \frac{2}{\Sigma} [\Delta\chi - a(\Sigma + a\chi) \sin^2 \theta], \quad (2.11)$$

$$g_{\varphi\varphi} = \frac{1}{\Sigma} [(\Sigma + a\chi)^2 \sin^2 \theta - \chi^2 \Delta]. \quad (2.12)$$

The above metric (2.7) describes a black hole, see figure 2.2. The horizon, the surface which cannot be crossed outward, is determined by the condition $g_{rr} \rightarrow \infty$. Therefore, using the expression (2.4), which is a quadratic

equation, it is possible to get the radial coordinate of the event horizon. Following the condition $\Delta(r) = 0$, we have the exact solution:

$$r_{\pm} = M \pm \sqrt{M^2 + l^2 - a^2}. \quad (2.13)$$

Now, from Eq. (2.13), it is possible to have the event horizon coordinate.

$$r_h = r_+ = M + \sqrt{M^2 + l^2 - a^2}. \quad (2.14)$$

In the same way, using the expression (2.8) and equal it to zero, it is possible to have the static limit, given by

$$r_{sta} = M + \sqrt{M^2 + l^2 - a^2 \cos^2 \theta}. \quad (2.15)$$

The region between the static limit (2.15) and (2.14) is known as the ergoregion. Within it, it is not possible to “stand still.” Generally, objects tend to move in the direction of the black hole rotation and arbitrary directions. Moreover, the most exciting thing is that objects can enter this region and escape to infinity^{24,37,38}.

Additionally, it is important to express in terms of dimensionless parameters. Setting, $a_* = \frac{a}{M}$ and $l_* = \frac{l}{M}$ (the fact suggests that a and l must have units of mass). Thus, equations (2.14), (2.15) are given as follows:

$$r_h = M \left(1 + \sqrt{1 + l_*^2 - a_*^2} \right), \quad (2.16)$$

$$r_{erg} = M \left(1 + \sqrt{1 + l_*^2 - a_*^2 \cos^2 \theta} \right), \quad (2.17)$$

Moreover, it is important to mention that to obtain the essential singularity we need to consider that $g_{tt} \rightarrow \infty$, which implies that $\Sigma = 0$ which is given by expression (2.5), it is possible to have the following results^{30,32,39}

$$r = 0 \quad \text{and} \quad \theta = \cos^{-1} \left(\frac{-l_*}{a_*} \right). \quad (2.18)$$

Now, it is important to mentioned that to have a black hole with singularity the condition that $a^2 \geq l^2$ or $a_* \geq l_*$ ^{30,39,40}, must be accomplished. Otherwise, we will have a regular black hole, which implies that it has no singularities (non-regular black holes have singularities)⁴¹. In that case, we do not care about the nature of the singularity, only in that case we assume that the metric describes a black hole with its corresponding event horizon.

Additionally, from Eq. (2.5) it is possible to determine the origin of the cosmic strings in the Kerr-Taub-Nut space-time. Implying that,

$$l + a \cos \theta = 0. \quad (2.19)$$

It is clear to see that at $\theta = 0$ and $\theta = \pi$, Eq. (2.19) implies that

$$l = a, \quad (2.20)$$

$$l = -a.$$

In that sense at $\theta = 0$ and $\theta = \pi$, it is possible to have a not well-behave axis, which can be explained due to the existence of the cosmic strings (see figure 2.2).

2.2 Dynamics of a Minimally Coupled Massless Scalar Field

In this part we review the Quantum Field Theory in a curved space, which is considered as the semiclassical approximation. It means that the fields are treated quantum mechanically while keeping the gravitational theory classical as in General Relativity.⁴²

Let us consider the theory of a massless Klein-Gordon scalar field ϕ in a curved space given by the metric $g_{\mu\nu}$ (2.7). The effect of gravity is included in the Klein-Gordon equation by upgrading the partial derivative to a covariant derivative $\partial_\mu \rightarrow \nabla_\mu$ ⁵. Therefore, the dynamics of a minimally coupled field to a specific space time is given by the following expression:

$$g^{\mu\nu} \nabla_\mu \nabla_\nu \phi = 0. \quad (2.21)$$

As the action of the covariant derivative on a scalar is the same as the action of the normal derivative. Then, Eq. (2.21) is expressed as follows:

$$g^{\mu\nu} \nabla_\mu \partial_\nu \phi = 0. \quad (2.22)$$

Recalling the following expression $\nabla_\mu V_\nu = \partial_\mu V_\nu - \Gamma_{\mu\nu}^\lambda V_\lambda$, the Klein-Gordon equation is rewrote in the following form*:

$$g^{\mu\nu} (\partial_\mu \partial_\nu - \Gamma_{\mu\nu}^\lambda \partial_\lambda) \phi = 0. \quad (2.23)$$

where $\Gamma_{\mu\nu}^\lambda$, are the Christoffel symbols defined as follows:

$$\Gamma_{\mu\nu}^\lambda = \frac{g^{\lambda\rho}}{2} (\partial_\mu g_{\nu\rho} + \partial_\nu g_{\rho\mu} - \partial_\rho g_{\mu\nu}). \quad (2.24)$$

The solution of Eq. (2.22) depends on the space-time which is considered to be analyzed. Regardless of the situation, a partial differential equation will always be obtained. In general, the most common method to solve this equation is applying the Separation of Variables Method, that makes the problem more tractable⁴³⁻⁴⁵. Therefore, the scalar field must be decomposed as follows:

$$\phi(t, r, \theta, \varphi) = e^{-i\omega t} R_{\ell m}(r) S_{\ell m}(\theta) e^{im\varphi}, \quad (2.25)$$

where ω , ℓ , and m denote the frequency of the i th emitted particle, spherical harmonic quantum number, and the axial quantum number, respectively⁴⁶. Moreover, $S_{\ell m}$ are spheroidal angular functions, $R_{\ell m}$ are the radial functions, which share indices due to their dependence on ℓ and m , $e^{-i\omega t}$ comes from the temporal solution of the Klein-Gordon equation, and $e^{im\varphi}$ from the azimuthal solution (i.e., depends on the azimuthal angle φ).

2.2.1 Effective Potential

In order to develop this part, it is important to consider the radial part of the differential equation (2.22), once the scalar decomposition is applied. The general idea is to obtain a Schrödinger-like wave equation. To do this, we need to apply a tortoise coordinate transformation to the radial part, $R_{\ell m}$ of the Klein-Gordon equation^{47,48}. In general,

*The equivalent form of the Klein-Gordon equation is given by: $\frac{1}{\sqrt{-g}} \partial_\mu (\sqrt{-g} g^{\mu\nu} \partial_\nu \phi) = 0$ ³⁰

the tortoise coordinate r_* allows an observer to see the objects reach and escape from the regions near the event horizon of the black hole³⁸. It means that the region outside the horizon of the black hole $r_h < r_* < \infty$ maps to $-\infty < r_* < +\infty$ ⁴⁹ which means that the horizon has been pushed to $-\infty$. Therefore, an observer is going to be able to detect the radiation that comes from the black hole, taking $-\infty$ as the source reference point.

For example, the tortoise coordinate r_* for a Kerr metric is given by the following expression:

$$\frac{dr_*}{dr} = \frac{r^2 + a^2}{\Delta}. \quad (2.26)$$

As it was mentioned before, the main idea of the coordinate change is to obtain a wave equation. In most of the cases, the differential equation looks as the following expression,

$$\frac{d^2 R_{\ell m}(r)}{dr_*^2} + (\omega^2 - V_{eff}) R_{\ell m}(r) = 0. \quad (2.27)$$

From Eq. (2.27), the most important thing is that we can identify the effective potential V_{eff} . This potential acts as a filter of the scalar field. It means that part of the field will go outside from the regions near the black hole horizon, and the rest will be reflected into the black hole* (see figure 2.3). Furthermore, it is essential to mention that there is no explicit mathematical expression to describe the effective potential since it depends on the nature of the space-time (i.e., black hole geometry). In general, the effective potential plays a crucial role in analyzing Hawking radiation, as we will see in the next section 2.3.

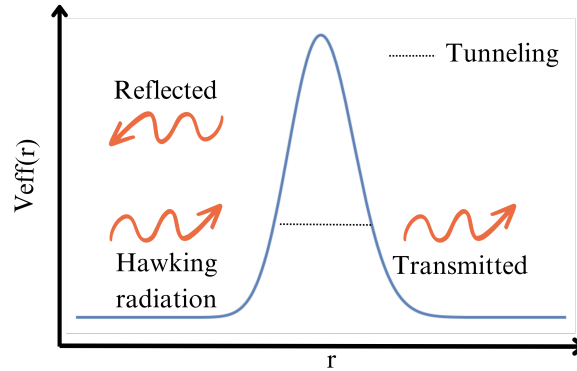


Figure 2.3: Effective potential mechanism sketch: part of the radiation will be transmitted and will travel freely to infinity, whereas another part will be reflected back into the hole.

*The field fluctuations could be considered particles.

2.3 Hawking Radiation

In 1975, Hawking applied the quantum theory near a black hole and found that they emit thermal radiation⁵⁰. Additionally, they have a temperature, leading to the Hawking radiation⁵¹. The radiation mechanism arises from the dynamic nature of the collapsing matter's internal geometry, leading to fluctuations in space-time. Consequently, the creation of particles in the vicinity outside the event horizon of a black hole is expected. Additionally, it is essential to consider that the number of particles (f) created in the regions near the event horizon of the black hole represents a black body radiation distribution, given by:

$$f = \frac{1}{e^{\frac{\omega}{T_H}} \pm 1}, \quad (2.28)$$

where ω is the frequency of the emitted radiation and T_H is the temperature associated with the black hole.

As a consequence of the quantum fluctuations from the regions near the black hole⁵², a pair of virtual particles is created, one of them with positive energy and the other with negative energy. The particle with negative energy falls into the black hole and the other particle escapes to infinity as Hawking radiation⁵³ (see figure 2.4).

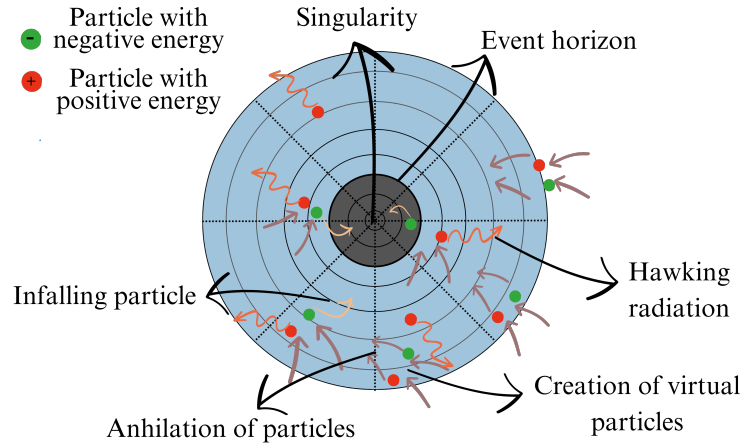


Figure 2.4: Hawking radiation mechanism.

2.3.1 Entropy and Thermodynamics

As we discussed before, black holes have a temperature as a consequence of Hawking radiation. In the same way they must have entropy. Therefore, the temperature and the entropy settled the basis of black hole thermodynamics⁵.

In general, the temperature of a black hole is given by the following expression

$$T_H = \frac{\kappa}{2\pi}, \quad (2.29)$$

where κ is the acceleration that a hypothetical test particle feels at the event horizon of a black hole, known as the surface gravity (see³⁷ for more details). Additionally, it is important to mention that black holes with small masses

have high temperatures in comparison with the massive ones. It is supported on the fact that if we consider the temperature for a Schwarzschild black hole

$$T_{BH} \approx \frac{1}{8\pi M}. \quad (2.30)$$

Therefore, it is possible to see that the relation between the black holes mass and their temperatures is inversely proportional^{37,53}.

If a black hole has temperature and energy, it must also have entropy. Before Hawking discovered that black holes emits particles, Bekenstein⁵⁴ argued that black holes must have an intrinsic entropy that is proportional to its area, although he did not manage to determine the constant of proportionality. After the discover of Bekenstein, Hawking⁵⁰ demonstrated the same formula including the fact that black holes must be treated as thermal objects obeying the laws of thermodynamics. As a consequence of this, the formula (2.31) is called the Bekenstein-Hawking entropy, defined as follows[¶]

$$S_{BH} = \frac{A}{4} \quad (2.31)$$

where A is the area of the black hole event horizon which can be calculated with the following expression:

$$A_H = \int_{r=r_h} \sqrt{g_{\theta\theta}g_{\phi\phi}} d\theta d\phi. \quad (2.32)$$

As the entropy obeys the thermodynamics law, it states that the horizon area of the black hole must be non-decreasing in any physically allowed process. Moreover, it counts the number of microstates of a black hole of a given size⁵⁵ or the degrees of freedom needed to describe a black hole.

$$dS \propto dA \geq 0. \quad (2.33)$$

However, as consequence of the Hawking mechanism the event horizon tends to disappear implying that entropy will decrease. So that, it apparently violates the second law of thermodynamics. In that sense Bekenstein established a generalized entropy that states that there could be a contribution from the matter outside the black hole horizon. Therefore, the generalized entropy is expressed in the following way

$$S_{gen} = S_{BH} + S_{outside} \geq 0. \quad (2.34)$$

Additionally, the generalized entropy (2.34) is also known as the coarse-grain entropy. A broad overview of a system involves simplifying or averaging out specific intricate details, as the observer lacks access to microscopic information and possesses only a limited, generalized understanding of the system. This form of description relies on the overarching features of the system, constituting a macroscopic perspective. Consequently, coarse-grained entropy measures the observer's incomplete knowledge about the system when information is restricted to a subset of macroscopic observables rather than the complete set of microscopic details. This entropy either increases or stays the same during a unitary time evolution under the consideration of a closed system^{3,5,55,56}.

[¶]See appendix B for its derivation.

2.3.2 Greybody Factors

In order to study the Hawking radiation, let us recall the use of the effective potential that we discussed in the subsection 2.2.1. As we studied before, the effective potential acts like a filter of a field (see subsection 2.2.1). In other works, the black hole geometry outside the event horizon acts as a potential barrier that filters Hawking radiation, i.e, part of the radiation will be transmitted and will go to infinity, whereas the rest will be reflected into the black hole⁵⁷.

Additionally, it is important to consider that the geometry of the space-time surrounding the black hole is non-trivial. It implies that once the Hawking radiation is emitted at the event horizon, the radiation will get modified due to the geometry of the space. If an observer is far from the black hole and wants to measure the radiation spectrum, it will no longer be a black body. So, the black holes will emit Hawking radiation as grey bodies instead of black bodies⁵⁸ (see. Figure 2.5).

In the scientific literature, it has been theoretically proven by Hawking (1975)⁵⁰ that black holes emit radiation, which renders them non-black and gives them a grey appearance. The observation of this radiation by an asymptotic observer differs from the original radiation near the black hole's horizon due to a redshift factor, referred to as the greybody factor^{59,60}. The greybody factor, or the absorption cross-section, is a frequency-dependent factor that measures the modification of the original blackbody radiation and gives us valuable information about the near-horizon structure of black holes⁶¹. Additionally, according to Pantig et al.⁶², greybody factors (GFs) measure a black hole's quantum nature. A high value of GFs indicates a high likelihood of Hawking radiation to be captured by the black hole^{59,63}. In other words, the previous fact indicates that less radiation is able to pass the potential barrier generated by the black hole (i.e., effective potential). For this reason, GFs of test fields are crucial in determining the intensity of Hawking radiation.

In general it means that Eq. (2.35) will be affected by the GFs as follows:

$$f = \frac{\gamma(\omega)}{e^{\frac{\omega}{T_H}} \pm 1}, \quad (2.35)$$

where $\gamma(\omega)$ is the greybody factor, and the use of the \pm sign depends on the nature of the particles that are going to be analyzed, for example it is usual to use $+$ for fermions and $-$ for bosons.

Now, in order to calculate the greybody factor $\gamma(\omega)$ which could be considered as the transmission probability for an outgoing wave emitted from the black hole horizon to reach the asymptotic region, we use the lower bound semi-analytic approach, which has been used to establish limits in the particle production in different space-times^{64,65}.

Therefore, the expression to calculate the GF is given by the following expression:

$$\gamma_{\ell m}(\omega) \geq \text{sech}^2 \left(\int_{-\infty}^{\infty} \vartheta dr_* \right), \quad (2.36)$$

where $\gamma_{\ell m}(\omega)$ is the greybody factor, and ϑ is the function:

$$\vartheta = \frac{\sqrt{(h')^2 + (\omega^2 - V - h^2)^2}}{2h}. \quad (2.37)$$

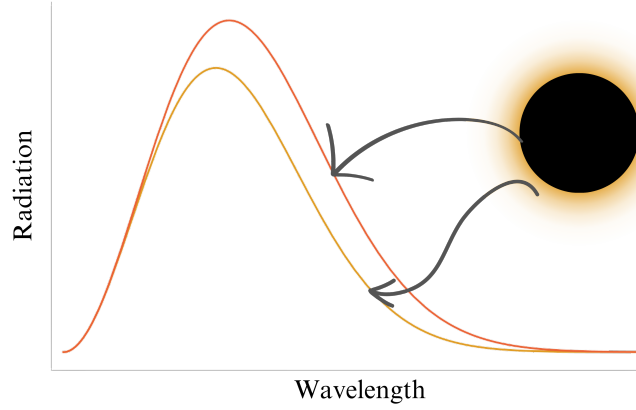


Figure 2.5: The non-trivial geometry of the space outside the black hole modifies the thermal radiation emitted at the horizon (reddish profile). Therefore, the black hole radiation spectrum is a modified blackbody radiation (orange profile).

Furthermore, h is some positive function, $h(r_*) > 0$, satisfying the limits $h(-\infty) = h(+\infty) = \omega$, and V is the effective potential taken from the Schrödinger-like wave equation (2.27).

Setting $h = \omega^{65}$, Eq. (2.36) turns into the following expression:

$$\gamma_{\ell m}(\omega) \geq \text{sech}^2 \left(\frac{1}{2\omega} \int_{-\infty}^{\infty} V(r_*) dr_* \right). \quad (2.38)$$

Finally, getting out from the tortoise coordinate system, the final expression for the GFs is the following:

$$\gamma_{\ell m}(\omega) \geq \text{sech}^2 \left(\frac{1}{2\omega} \int_{r_H}^{\infty} V(r) dr \right). \quad (2.39)$$

The expression (2.39) is the main equation that allows the calculation of the GF for different space-times.

2.3.3 Emission Rates

The black hole emission spectrum depends crucially on the structure and dimensionality of the embedding space-time. This means that Hawking radiation is linked to the parameters that describe the space-time. For example, in the case of a Kerr black hole, radiation will depend on the evolution of the black hole's mass and angular momentum.

The black hole emission or differential decay is given by the Hawking formula^{5,50,66-68}:

$$\frac{dE(\omega)}{dt} = \sum_{\ell m} \gamma_{\ell m}(\omega) \frac{\omega}{\exp(\omega/T_{BH}) \mp 1} \frac{d^{n+3}k}{(2\pi)^{n+3}}. \quad (2.40)$$

The above equation can be manipulated in $3 + n$ dimensions (i.e., It is a generalized formula). Additionally, it is important that in the phase-space, $k = \omega$, so that, the energy emission is given by the following expression⁶⁹:

$$\frac{d^2 E(\omega)}{d\omega dt} = \frac{1}{2\pi} \sum_{\ell m} \gamma_{\ell m}(\omega) \frac{\omega}{\exp(\omega/T_{BH}) \mp 1}. \quad (2.41)$$

Moreover, expression (2.40) can be generalized to get the fluxes or emission rates for the number of particles N , mass M , angular momentum J , and charge Q as follows⁷⁰:

$$\frac{d^2 \{N, M, J, Q\}}{d\omega dt} = \frac{1}{2\pi} \sum_{\ell m} \gamma_{\ell m}(\omega) \frac{\{1, \omega, m, q\}}{\exp(\omega/T_{BH}) \mp 1}. \quad (2.42)$$

The Eq. (2.42) will be used later in order to include the emission rate for the nut parameter l .

2.3.4 Black hole evaporation and Information Loss Paradox

One of the primary implications of the Hawking radiation is the eventual evaporation of black holes, as illustrated in Figure 2.6. While it is widely acknowledged that the mass of a black hole must be positive, the phenomenon of pair production introduces a propensity for mass loss. In this scenario, when a particle with negative energy falls into the black hole, it contributes negatively to the mass of the black hole, as discussed by Schutz⁵³.

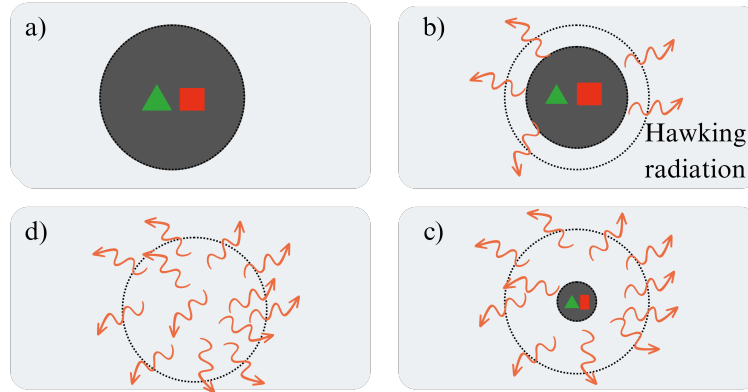


Figure 2.6: Stages of black hole evaporation.

In figure 2.6, the evaporation process of a black hole is described. In the first stage, a), once the black hole is created after the collapse star. Inside the black hole the geometry of the space-time continues to elongate in one direction while pinching toward a zero size singular point. Additionally, it is essential to mention that the initial state of the black hole contains information about the parent star and the matter that was swollen. That information is represented by geometric figures (red, green). In the second stage, b), the Hawking process creates entangled pairs of particles, one trapped by the hole and the other one escaping to infinity, where it is observed as Hawking radiation.

The black hole slowly shrinks in the next stage, c) as the radiation carries away its mass. The process continues until the size of the event horizon tends to zero. At the final stage, d) there is a smooth space-time containing thermal Hawking radiation, but there is no a black hole anymore.

It is commonly known that black holes swallow up lots of information. Since they refuse to tell us what has fallen in, they are systems which have the same external state for lots and lots of possible internal states⁵³, but once the black hole evaporates, what happen with the information inside the black hole? This fact leads to the **information loss paradox**.

In the classical framework, an observer never perceives an object crossing the event horizon because time slows down near the horizon. This implies that everything will eventually be observed, and there will be no information loss. However, when delving into the quantum theory, a different narrative emerges—objects disappear, and we are left without information about them. In general, information loss arises due to quantum effects, but this conflicts with the unitary evolution in quantum mechanics³⁷.

The Hawking information paradox is generally an argument against the central dogma. The idea of the dogma relies on the fact that, as seen from the outside, a black hole can be described as a pure quantum system, see figure 2.7, which evolves unitarily under time evolution^{5,51}. Hawking argued that if we see a black hole as a pure quantum system, it must evolve into a mixed state. This fact represents a break of unitarity since we start with a pure state, which is entirely determined, and we end up with a mixed state, which is not completely determined; information is lost in black hole evaporation⁵.

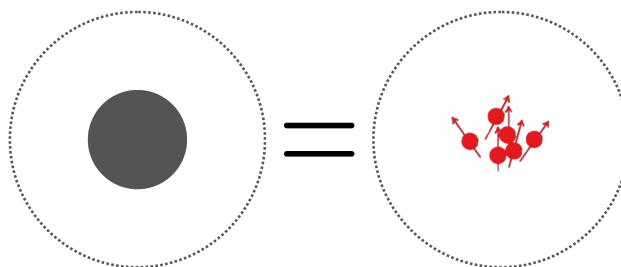


Figure 2.7: The black hole and the whole spacetime around it, up to some surface denoted by the dotted circle, can be replaced by a quantum system. This quantum system interacts with the outside via a unitary mechanism.

2.4 The Page Curve

2.4.1 The Fine-Grained Entropy

A detailed system description is thorough and accurate, revealing exactly how it is configured on the inside. This description comes from understanding the tiny behaviors of its individual parts or microstates. The fine-grained entropy tells us how much the observer does not know about the system when the observer has complete information about all the tiny details. Moreover, interestingly, this measure stays the same as time passes, which implies that it is invariant under unitary evolution^{3,5,55}. Moreover, as the coarse-grained entropy (2.34), it works under the assumption of a close system.

Additionally, the fine-grained entropy is also known as the entanglement entropy or the Von Neumann entropy, which measures the degrees of freedom, or more roughly, our incomprehension about a quantum state⁵. Which is defined as follows

$$S_{VN} = -Tr(\rho \log \rho), \quad (2.43)$$

where ρ is the density matrix of the quantum states with dimensions of the Hilbert space \mathcal{H} of the quantum system.

When a black hole emits Hawking radiation, the particles that escaped from the event horizon are entangled with the ones that fell into the black hole such that every pair forms a pure quantum state $|\psi_a\rangle$ that lives in \mathcal{H} , the infinite dimensional Hilbert space. Additionally, the density matrix for a pure state is defined by

$$\rho_{pure} = |\psi_a\rangle \langle \psi_a|. \quad (2.44)$$

Now, it is possible to create mixed quantum states as a collection of pure quantum states, whose density matrix is given as follows

$$\rho_{mixed} = \sum_a p_a |\psi_a\rangle \langle \psi_a|, \quad (2.45)$$

where p_a represents the probabilities of each pure state in the collection. In general, the density matrix is useful to describe thermal systems, in that case the Hawking radiation.

Now, considering an operator U that acts on the elements of \mathcal{H} in this way $|\psi_b\rangle = U |\psi_a\rangle$ such that $\langle \psi_b| = \langle \psi_a| U^\dagger$. Given that $\langle \psi_i | \psi_j \rangle = \delta_{ij}$, we get that

$$1 = \langle \psi_b | \psi_b \rangle = \langle \psi_a | U^\dagger U | \psi_a \rangle \Rightarrow U^\dagger U = 1.$$

Practically, it implies that when a pure quantum state evolves under a unitary operator U the final result is the same state, so that, when the entanglement entropy is calculated it must evolve to zero^{3,5,57}.

Now, taking into account that black hole radiation has a thermal nature it implies that a pure quantum state evolves into a mixed one, which implies that

$$\rho_{mixed} \neq U \rho_{pure} U^\dagger. \quad (2.46)$$

In other words, a pure state cannot evolve into a mixed state under unitary evolution (i.e., a pure state must evolve into a pure one under unitarity). Therefore, the Hawking radiation constitutes a breakdown of unitarity, which carries out

another version of the information paradox^{3,5}. Additionally, it implies that when more and more Hawking radiation is emitted; the entanglement entropy increases and does not tend to zero.

2.4.2 Correlation between the Black Hole and its Radiation

At this point, we have discussed that the fine-grained entropy of the radiation implies that the information is not conserved. Generally, it happens because the entanglement is considered only between the pair of particles, so that the Hawking radiation has nothing to do with black hole information^{3,5}. Additionally, the unitarity condition breaks down.

The main question of the information paradox is whether the processes of formation and evaporation of a black hole can be described unitarily. In order to solve the problem, it is important to consider that the black hole and the radiation are two entangled subsystems that form a pure quantum state. Therefore, during the evaporation process of a black hole, the entropy of the radiation and the entropy of the black hole (Bekenstein-Hawking entropy) must be the same

$$S_{rad} = S_{BH}. \quad (2.47)$$

Moreover, it is important to consider that the black hole and its radiation are correlated under the condition that the fine-grained entropy must be less than the coarse-grained entropy or in simple way; the Bekenstein-Hawking entropy

$$S_{rad} \leq S_{BH}. \quad (2.48)$$

The above condition must be accomplished, otherwise it would not be possible for the radiation to be entangled with the black hole, since the black hole would not have enough degrees of freedom⁵.

In summary, it implies that when the black hole is being evaporated the thermodynamic entropy given by the Bekenstein-Hawking formula (2.31) (green line, figure 2.8) is decreasing due to the shrinking of the event horizon. At the same time, the entropy of the radiation is increasing (orange line, figure 2.8). It implies that at some point both entropies will meet, and the condition (2.48) will be violated. This cannot occur since the number of degrees of freedom of the black hole is related to the thermodynamic entropy, so that, the entropy of radiation cannot be more than this. This means that the entropy of radiation must begin decreasing at this point and continue to decrease to zero when the black hole completely evaporates³¹. Suggesting the the black hole evaporation is a unitary process.

In 1993, Page⁴ proposed that if the black hole evaporation is a unitary process, then, the entanglement entropy between the outgoing radiation and the quantum state associated to the black hole is expected to follow the Page curve (blue line, figure 2.8)^{3,71,72}. Additionally, the time at which the Page curve turns over is called the Page time¹⁶.

The Page curve supports the idea that if a black hole is created through the collapse of matter in a pure state, then the black hole must also be in a pure state, and therefore, its Von Neumann entropy must be zero at the end of the evaporation. Moreover, it suggests that the information is conserved, implying a possible solution to the information loss paradox⁷. Additionally, it is essential to mention that Page time occurs when the coarse-grained entropy of the black hole is equal to the fine-grained entropy of the radiation; at this moment, the mass of the black hole is approximately half the original⁷³. After the Page time, there will be more energy in the form of Hawking radiation than there will be mass inside the black hole.

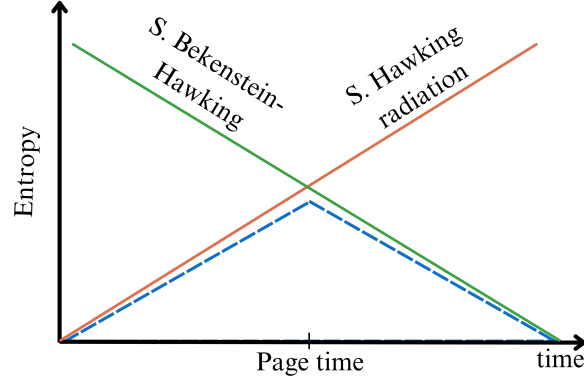


Figure 2.8: (For illustrative purposes) The green line is the black hole entropy given by the Bekenstein-Hawking formula (2.31). The orange line is the Hawking radiation entropy. The blue curve is the Page curve, the curve that the radiation entropy should follow if unitary time evolution is conserved. The time at which it turns over is called the Page time.

2.4.3 The Time Dependence of the Von Neumann Entropy

From the previous section, it is clearly to see that the Page curve practically is the plot of the Von Neumann entropy respect to time. It implies that it is necessary to implement the time dependence of the Bekenstein-Hawking and Hawking radiation entropies. In that sense, the time evolution of the parameters that describe the black hole is needed.

In order to do that it is important to consider the particle emission rates of the Hawking radiation which were discussed in subsection 2.3.3 and the method used by Page¹⁶ and Nian¹⁷, which can be generalized as follows⁷⁶.

$$\alpha = -M^3 \frac{d \ln H}{dt}. \quad (2.49)$$

Eq. (2.49) is known as the Page model for the particle emission rates⁷⁷, where H represents the parameter that needs to be considered for time evolution. Moreover, the luminosity or total power emitted is proportional to M^{-2} . As M decreases at this rate⁴⁶, the black-hole lifetime will be proportional to M^3 , which is the term that appears in Eq. (2.49).

Depending on the parameters that need to be analyzed, model (2.49) gives an ordinary differential equation for each black hole parameter (mass, angular momentum, and nut parameter). Each of the equations is coupled with each other due to the mass that will appear in every case. Finally, to obtain the required time evolution of the parameters, the system of differential equations formed by the differential equations that describe the evolution of each parameter needs to be solved. Additionally, it is important to mention that the methods used by Nian and Page were used to represent Kerr and Schwarzschild's black holes, respectively. Moreover, model (2.49) will be modified in the next chapter to have the nut parameter's time evolution.

Table 2.1: Summary of the entropies presented in the thesis.

Coarse-grained entropy	Fine-grained entropy
Measures the observer's incomplete knowledge about the system when information is restricted to a subset of macroscopic observables rather than the complete set of microscopic details.	Tells us how much the observer does not know about the system when the observer has complete information about all the tiny details.
Bekenstein-Hawking entropy	Von Neumann entropy = Entanglement entropy
<ul style="list-style-type: none"> • Measures of the total number of degrees of freedom available to the system. • Identifies and counts a specific set of microscopic states associated with the parameters describing the macroscopic black hole. It is possible to identify the states with those of infalling matter inside the black hole⁷⁴. • The entropy of the black hole measures the uncertainty concerning which of its internal configurations are realized. • It expresses our uncertainty in knowledge of black hole precise configuration. 	<ul style="list-style-type: none"> • It is defined as the fine-grained entropy of a quantum system. • It measures the degrees of freedom, or more roughly, our incomprehension about a quantum state. • It we consider a black hole and its radiation as a single quantum state, which is composed of the hole quantum system (A) and the radiation quantum system (B). The entropy is a measure of the degree of entanglement between A and B. For this reason, the Von Neumann entropy is also known as the entanglement entropy^{1,75}. • The entropy measures the mixture of the subsystem A (radiation) with the rest of the system.

Chapter 3

Results & Discussion

In this chapter we are going to apply the theoretical aspects discussed in the previous chapter in order to obtain the Page curve for a Kerr-Taub-Nut black hole.

3.1 Thermodynamics for a Kerr-Taub-Nut Black Hole

Let us recall the use of the metric that describes the space-time.

$$ds^2 = -\frac{1}{\Sigma}(\Delta - a^2 \sin^2 \theta) dt^2 + \frac{2}{\Sigma}[\Delta \chi - a(\Sigma + a\chi) \sin^2 \theta] dt d\varphi + \frac{1}{\Sigma}[(\Sigma + a\chi)^2 \sin^2 \theta - \chi^2 \Delta] d\varphi^2 + \frac{\Sigma}{\Delta} dr^2 + \Sigma d\theta^2.$$

3.1.1 Temperature

As we discuss before, as a consequence of the Hawking radiation, black holes must have a non-zero temperature. In this case, we calculate the temperature for a KTN black hole. In order to this, we need to use Eq. (2.29), and the surface gravity calculation provided by Siahhan⁷⁸. Therefore the surface gravity for a KNT black hole has the following expression:

$$\kappa = \frac{r_+ - r_-}{2(r_+^2 + a^2 + l^2)}, \quad (3.1)$$

where r_+ and r_- (expressions (2.13)) are the outer and inner horizons of the black hole, respectively. So that, temperature is described as follows:

$$T_{KTN} = \frac{r_+ - r_-}{4\pi(r_+^2 + a^2 + l^2)}. \quad (3.2)$$

If we replace the expressions (2.13) in Eq. (3.2), we can get the temperature of the KNT black hole, which is

expressed as follows*:

$$T_{KTN} = \frac{\sqrt{M^2 + l^2 - a^2}}{2\pi \left[\left(\sqrt{M^2 + l^2 - a^2} + M \right)^2 + a^2 + l^2 \right]}. \quad (3.3)$$

After some manipulations of Eq. (3.3) and using International system units, it is possible to have the following expression for the temperature of a KTN black hole.

$$T = \frac{\hbar c^3}{2\pi G k_B M_\odot} \frac{\sqrt{1 + l_*^2 - a_*^2}}{\left[\left(\sqrt{1 + l_*^2 - a_*^2} + 1 \right)^2 + a_*^2 + l_*^2 \right]} \left(\frac{M_\odot}{M} \right) [K], \quad (3.4)$$

where $k_B = 1.381 \times 10^{-23} \text{ J/K}$, $G = 6.674 \times 10^{-11} \frac{\text{N m}^2}{\text{kg}^2}$, $\hbar = 1.055 \times 10^{-34} \text{ J s}$, $c = 2.998 \times 10^8 \text{ m/s}$, and M_\odot is the solar mass.

Note that Eq. (3.4) is subject to the restriction $a_*^2 - l_*^2 \leq 1$.

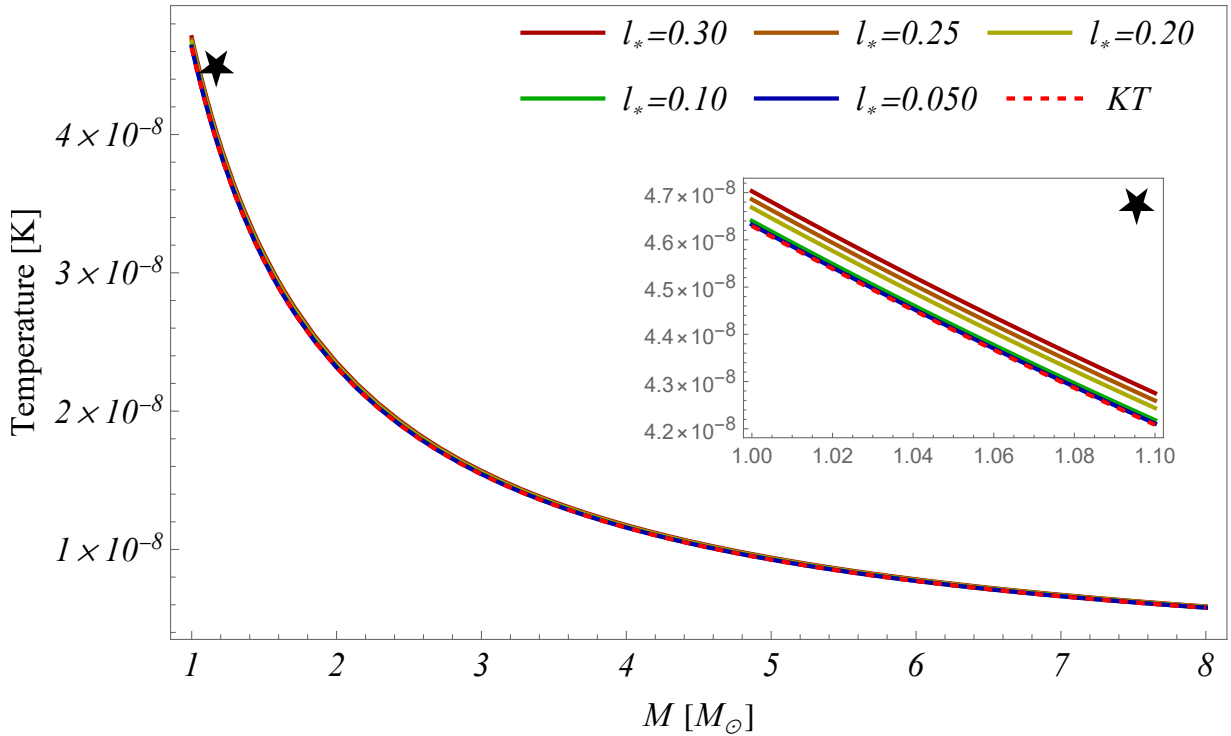


Figure 3.1: Temperature for a Kerr-Taub-Nut black hole that depends on the mass M expressed in solar masses, we set the rotation parameter $a_* = 0.8$ (considering that black holes have significant rotation, a_* near to 1) and for different nut values l_* .

*Note that this expression reduces to the temperature of a Schwarzschild black hole when $a \rightarrow 0$ and $l \rightarrow 0$

From the small window of figure 3.1, where we consider the range $1 - 1.1 M_{\odot}^*$, it is clear that the nut parameter affects the temperature of the black hole. If we see the red dashed line, which represents the Hawking temperature of a Kerr black hole, it is evident that when the nut parameter tends to zero, the temperature of the KTN black hole tends to the Kerr temperature (KT). Thus, the presence of a high value for the nut parameter implies an increase in temperature for low-mass black holes.

Additionally, it is essential to mention that the trend outside the window from Fig. 3.1 is the same as from regions outside it. Considering the mass of different black holes, it is noticeable that massive holes have lower temperatures than less massive black holes (low-mass: 1 to $3 M_{\odot}$, high-mass: 4 to any order of solar masses), which possess high temperatures. The previous fact is consistent with the ideas discussed in subsection 2.3.1 since the temperature is in order of 10^{-8} implies that the spectrum for the black holes is localized in the long wavelength regimen ($\approx 10^5 m$) (i.e., Wien's displacement law). Additionally, the lower the black hole mass, the higher the temperature and the more particles emitted by the black hole. In this case, black holes could be considered unstable systems with no equilibrium point⁷³, which means that there is a change in temperature between the emission of subsequent particles; for this reason, we set the lower mass limit $M = 1 M_{\odot}$

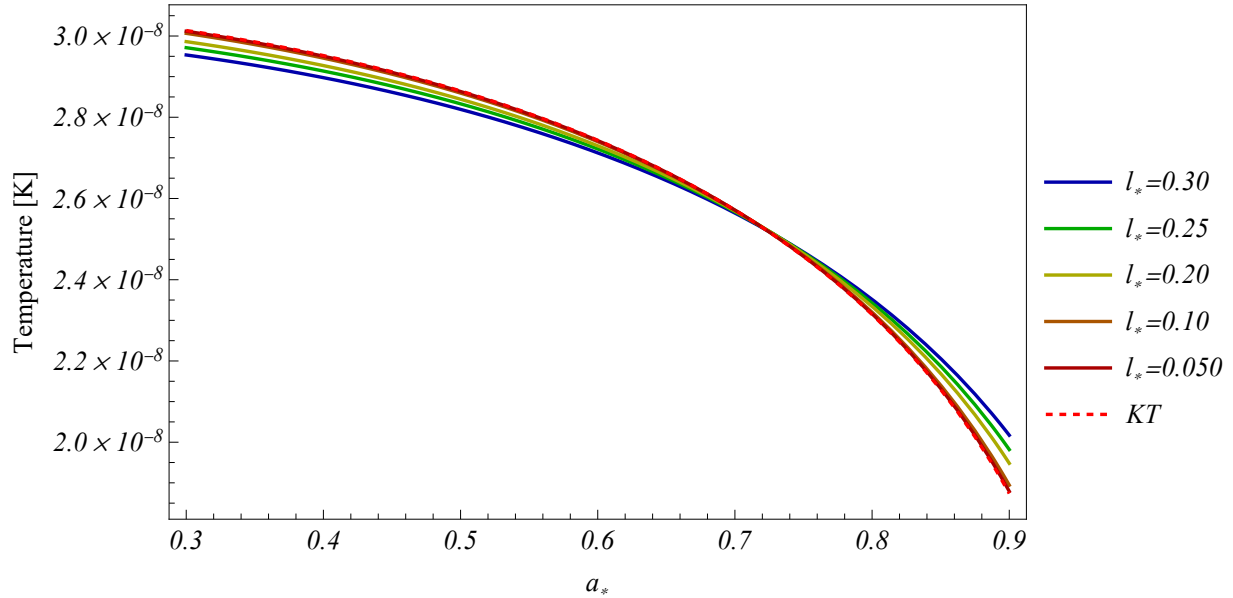


Figure 3.2: Temperature for a Kerr-Taub-Nut black hole that depends on the rotation parameter a_* , we set the mass $M = 2 M_{\odot}$ and for different nut values l_* .

Figure 3.2 represents the relation between the temperature and the rotation parameter when the mass of the black hole is fixed. Additionally, it is clear that when both the rotation parameter and the nut parameter are small, the KTN black hole is characterized as having high temperatures similar to KT (i.e., Kerr black hole temperature). In

*The trend presented in the window is the same, if we work with another range of black hole masses

other words, the black hole emits much more particles as Hawking radiation than when high values of rotation and nut parameters are considered. In contrast, when the nut parameter is more significant, and the rotation parameter increases, the black hole does not emit much thermal radiation due to the apparent decrease in temperature. To summarize, the nut parameter reduces the emission of radiation for any choice, and it is as if an increase in the nut parameter contributes to slowing down the radiation process. Nevertheless, at rotations $a_* \approx 0.7 M_\odot$ the effect of the nut parameter dominates the temperature.

3.1.2 Bekenstein-Hawking Entropy

In order to quantify the knowledge about the Kerr-Taub-Nut black hole, it is necessary to calculate the entropy associated to the black hole. For this purpose of use the formula (2.31) and calculate the entropy, let us use Eq. (2.32) and the corresponding elements of the metric (2.7); considering that at the event horizon $\Delta(r_+) = 0$. So that,

$$A_{KTN} = \int_0^{2\pi} \int_0^\pi (\Sigma + a\chi) \sin \theta d\theta d\phi = 4\pi(\Sigma + a\chi). \quad (3.5)$$

Therefore, taking the previous result (Eq. (3.5)), the entropy is given by the following expression:

$$S_{KTN} = \pi(\Sigma + a\chi) = \pi(r_+^2 + l^2 + a^2). \quad (3.6)$$

Now, the most specific expression for the entropy (3.6) is:

$$S_{KTN} = 2\pi(M^2 + l^2 + M\sqrt{M^2 + l^2 - a^2}). \quad (3.7)$$

Table 3.1: Bekenstein-Hawking entropy for a Kerr-Taub-Nut, Kerr, and Schwarzschild black holes.

Mass $M [M_\odot]$	Rotation parameter $a [M_\odot]$	Nut parameter $l [M_\odot]$	Kerr-Taub-Nut $\frac{S}{M_\odot^2}$	Kerr $\frac{S}{M_\odot^2}$	Schwarzschild $\frac{S}{M_\odot^2}$
1	0.4	0.30	1.2908×10^1	1.2042×10^1	1.2566×10^1
2	0.5	0.25	3.7496×10^1	3.6901×10^1	3.7699×10^1
3	0.6	0.20	7.4635×10^1	7.4256×10^1	7.5398×10^1
4	0.7	0.10	1.2421×10^2	1.2411×10^2	1.2566×10^2
5	0.8	0.050	1.8650×10^2	1.8647×10^2	1.8850×10^2
3	0.4	0.050	7.4917×10^1	7.4893×10^1	7.5398×10^1
7	0.9	0.50	3.5167×10^2	3.4930×10^2	3.5186×10^2
10	0.3	0.20	6.9125×10^2	6.9087×10^2	6.9115×10^2

Upon analyzing the data presented in Table 3.1, distinct characteristics regarding entropy become apparent. Firstly, it is noteworthy that the entropies for the three black holes exhibit a notable similarity, implying a comparable level of complexity in studying each black hole. Additionally, when considering the entropy of the Schwarzschild

black hole, which is solely contingent on its mass, one might infer that the number of microstates for the black hole is predominantly influenced by its mass.

In essence, the observation suggests that the complexity associated with studying any of these black holes is akin. This uniformity arises from the fact that describing each black hole entails approximately the same number of degrees of freedom, which are estimated using the area of the black hole.

3.2 Massless Scalar Field in Kerr-Taub-Nut Space-Time

As we discussed before, the main step to understand the Hawking radiation is the derivation of the effective potential that the perturbations (massless particles) of the scalar field will feel.

In order to get the effective potential, let us start using Eq. (2.22) and the decomposition (2.27). In most of the cases it is essential to use the Teukolsky equation⁴⁵, which is very important to understand the Kerr black holes perturbations^{45,76,79}. The radial part of this equation is described as follows⁷⁹:

$$\frac{1}{\Delta^s} \frac{d}{dr} \left(\Delta^{s+1} \frac{dR_{\ell m}}{dr} \right) + \left[\frac{K^2 - 2is(r-M)K}{\Delta} + 4is\omega r - \lambda_{\ell m} \right] R_{\ell m} = 0, \quad (3.8)$$

where Δ is a function that comes from the metric, K is the wavenumber of the perturbation, and s is the spin weight of the field, which characterizes the intrinsic rotation of the field, and takes the values 0, 1 or 2 for scalar, electromagnetic or gravitational perturbations⁸⁰.

As we will work with scalar perturbations, it is essential to use a spin weight $s = 0$. Moreover, considering the wavenumber used by Yang et al.³⁰, Eq. (3.8), which represents the radial part of the perturbations for a KTN black hole, will be given by the following equation

$$\frac{d}{dr} \left(\Delta \frac{dR_{\ell m}}{dr} \right) + \left(\frac{K^2}{\Delta} - \lambda_{\ell m} \right) R_{\ell m} = 0, \quad (3.9)$$

where $\lambda_{\ell m}$ is the separation constant and is given by $\ell(\ell + 1) + O(a^2\omega^2)$ ⁸⁰, Δ is given by (2.4) and

$$K = \omega(r^2 + l^2 + a^2) - a m. \quad (3.10)$$

It is noteworthy to emphasize that leveraging the radial component of the Teukolsky equation enables a more efficient representation of the radial portion of the Klein-Gordon equation (2.22) governing the scalar field. This strategic utilization facilitates a faster analysis and modeling of the scalar field's radial behavior. Furthermore, we tailor this equation to our specific metric, capitalizing on the Kerr-like nature of our space-time. This adaptation ensures a more precise and contextually relevant application of the equations in the description of the scalar field dynamics within our space-time framework.

3.2.1 Effective Potential

Once we have the radial part of the perturbation, let us use Eq. (3.9) in order to calculate the effective potential.

First of all, it is important to obtain the Schrödinger-like wave equation, for this let us consider the following change of variable

$$R_{\ell m} = \frac{W}{\sqrt{r^2 + a^2 + l^2}}, \quad (3.11)$$

and the tortoise coordinate

$$\frac{dr}{dr_*} = \frac{\Delta}{(r^2 + a^2 + l^2)}. \quad (3.12)$$

After applying the above conditions to Eq. (3.9), we got the following Schrödinger-like wave equation for a KTN black hole, which is given by the following expression

$$\frac{d^2 W(r_*)}{dr_*^2} + (\omega^2 - V_{eff}) W(r_*) = 0, \quad (3.13)$$

where the effective potential for a KTN black hole in an massless scalar field V_{eff} is expressed as follows;

$$V_{eff} = V_{\omega \ell m}(r) = \frac{2 a m \omega}{a^2 + l^2 + r^2} - \frac{a^2 m^2 - \ell(\ell + 1)\Delta}{(a^2 + l^2 + r^2)^2} - \frac{\Delta r - \Delta(2r^2 - 2Mr) - \Delta^2}{(a^2 + l^2 + r^2)^3} - \frac{2\Delta^2 r^2}{(a^2 + l^2 + r^2)^4}. \quad (3.14)$$

In general, Eq. (3.14) represents the potential that the massless scalar field perturbations (bosons) will feel in the background of the black hole.

In figure 3.3 it is possible to see different profiles for the effective potential (3.14) in terms of the tortoise coordinate r_* which allow us to analyze the behavior of the effective potential using different parameters. Firstly, it is important to say the asymptotic behaviour of the potential at ∞ and $-\infty$ is zero, which guarantees that we can approximate the solutions of the Eq. (3.9) as a combination of outgoing and ingoing waves to the black hole horizon^{81,82}. However, we are not interested in this fact because we are going to use the potential to calculate the GFs instead of the wave solutions. Another important aspect of the potential is that it looks like a composition of Gaussian-like shapes which is a characteristic of asymptotically flat space-times⁸¹.

Another essential feature of the effective potential (3.14) is that the nut parameter is related to the height of the potential. Additionally, as the event horizon is at the negative infinity, and considering that particles arise from the right side of the potential, they will reach the first hill of the barrier (i.e., particles move from the right to the left). After that, particles must pass the tallest hill before reaching the event horizon and falling into the black hole. For low values of the nut parameters, it is clear that the intensity of the potential increases, and for high values of the nut parameter, the potential decreases. Now, if we consider the value of the rotation parameter, it is noticeable that for slow rotations, the potential is intense, peaked, and narrow Fig 3.14 (a). Those characteristics imply particles can escape to infinity as Hawking radiation due to difficulty reaching the event horizon. Moreover, the asymmetry of the potential is a consequence of the non-trivial geometry of the space generated by the black hole. On the other hand, when the rotations increase, it is possible to see that the intensity and narrowness decrease; this aspect contributes to the smoothness of the potential profile Fig. 3.14 (b), (c). Finally, if we consider a maximally rotating KTN black hole Fig. 3.14 (d), it is possible to identify a smooth potential with low intensity compared to the other situations.

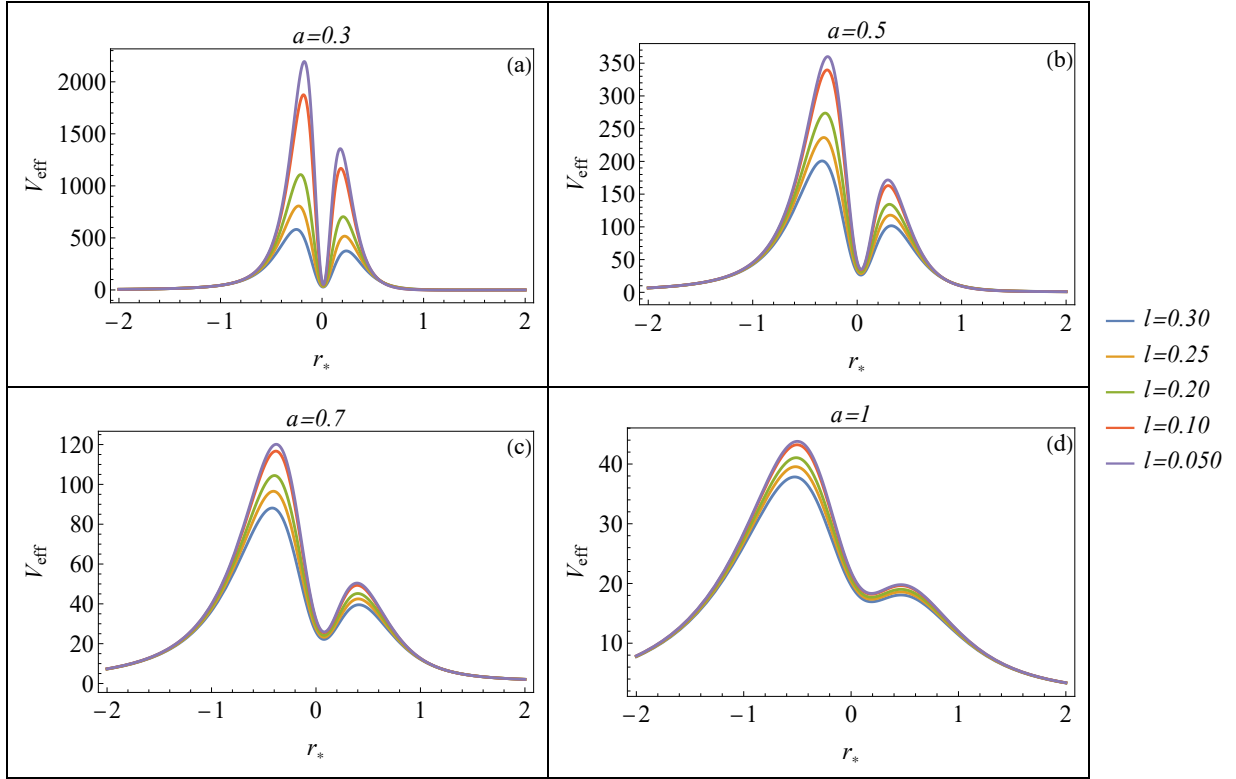


Figure 3.3: Plots of V_{eff} (3.14) for various values of the nut parameter l and rotation parameter a . Here the parameters are $M = 4$, $\omega = 10$, $\ell = m = 1$ (l and a are in solar masses).

Moreover, when the rotation increases, the peaks get broader. In general, it is possible to say that when both the rotation and the nut parameter of the black hole increase, the potential gets less intense and smooth, which increases the black hole's ability to capture particles⁸³, allowing them to escape with difficulty from the event horizon than when the nut parameter and the rotation parameter are small.

3.2.2 Effective potential at the horizon

In the previous section we discuss the effective potential that a Kerr-Taub-Nut black hole covering the space that goes from the event horizon to infinity, but it is important to consider the potential specifically at the event horizon. In order to get this potential, we are going to use the expression that we obtained previously (3.14) and considering that at the horizon $\Delta(r) \rightarrow 0$. Therefore, the potential is given as follows:

$$V_{horizon} = V_{\omega m}(r) = \frac{2 a m \omega}{a^2 + l^2 + r_h^2} - \frac{a^2 m^2}{(a^2 + l^2 + r_h^2)^2}, \quad (3.15)$$

where m is the axial quantum number and r_h is the event horizon of the KTN black hole. If Eq. (2.14) is replaced into Eq. (3.15), it is possible to have the potential at the horizon in terms of the mass. Therefore,

$$V_{horizon} = V_{\omega m}(r) = \frac{2 a m \omega}{a^2 + l^2 + (M + \sqrt{M^2 + l^2 - a^2})^2} - \frac{a^2 m^2}{\left[a^2 + l^2 + (M + \sqrt{M^2 + l^2 - a^2})^2 \right]^2}, \quad (3.16)$$

Now, combining equations (3.15) and (3.13), we have a new representation for the Schrödinger-like wave equation given by;

$$\frac{d^2 W(r_*)}{dr_*^2} + \left[\omega - \frac{a m}{(a^2 + l^2 + r_h^2)} \right]^2 W(r_*) = 0, \quad (3.17)$$

where $\left[\omega - \frac{a m}{(a^2 + l^2 + r_h^2)} \right]^2$ could be defined as a the effective potential at the event horizon. Thus,

From figure 3.4, it is possible to identify that the black hole's rotation affects the potential at the event horizon. When the black hole tends to its maximum rotation, the potential is less than when the rotation decreases. Therefore, the relation between rotation and the potential is inversely proportional. In the same way, the less massive black holes have a weak potential compared to the massive BHs. Another important fact is that the potential tends to be constant at a certain mass, which means it does not matter if we continue increasing the mass; the particles will feel the same potential.

Additionally, from the above equation (3.17), it is possible to define the angular velocity of the KTN black hole Ω_{KTN} as:

$$\Omega_{KTN} = \frac{a}{a^2 + l^2 + r_h^2}, \quad (3.18)$$

which is in agreement with the work of Yang et.al³⁰. Therefore, Eq. 3.17 can be written in the following form

$$\frac{d^2 W(r_*)}{dr_*^2} + (\omega - \Omega_{KTN} m)^2 W(r_*) = 0, \quad (3.19)$$

and the solution of the differential equation (3.19) is

$$W(r_*) \sim \exp[\pm i(\omega - m \Omega_{KTN}) r_*]. \quad (3.20)$$

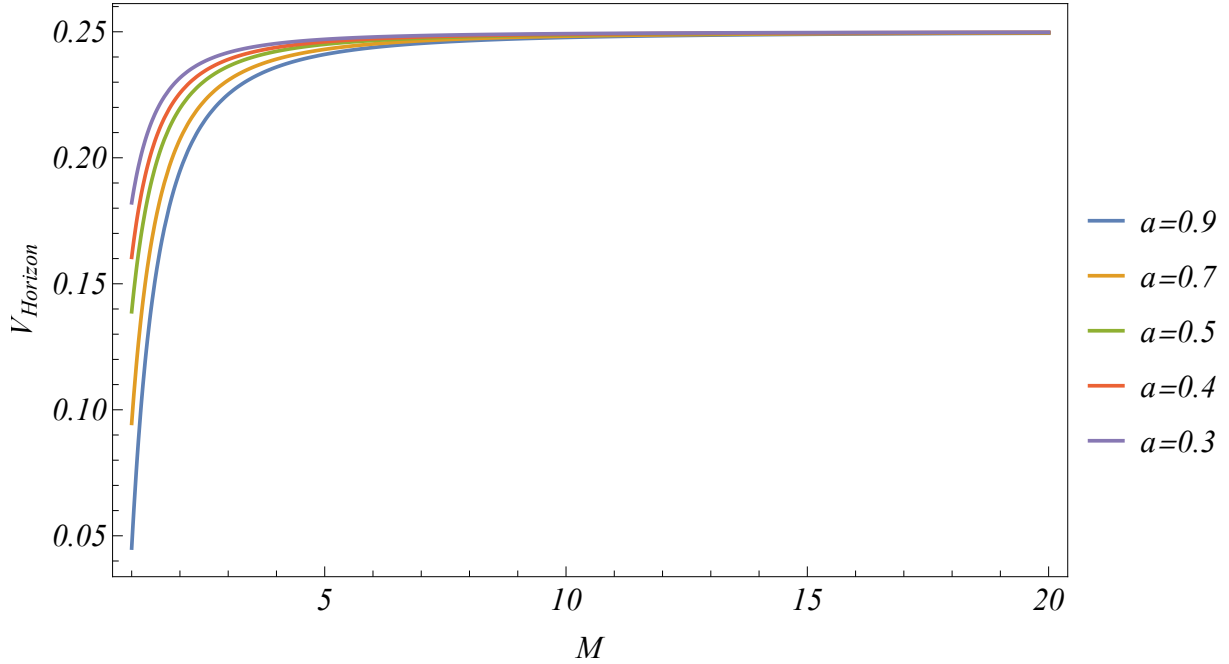


Figure 3.4: Plots of the effective potential at the event horizon $V_{horizon}$ given by expression (3.16) for various values of the rotation parameter a (in solar masses). Here, we set $m = 1$, $l = 0.25 M_{\odot}$.

It is clear that solution (3.20) represents waves. The plus and minus signs represent the outgoing and incoming wave modes, perturbations, or particles that arise from the massless scalar field, respectively. In general, this solution implies that at the horizon some particles can escape and others fall into the black hole. Thus, this is the origin of the Hawking radiation, which will be discussed in next section.

3.3 Hawking Radiation for a KTN Black Hole

As we discussed before, the black holes emit radiation as greybodies as a consequence of the grey-body factors that modify the black-body nature of the Hawking radiation spectrum. For this reason, in this section we calculate the grey-body factors for a Kerr-Taub-Nut black hole.

3.3.1 Gray Body Factor

Once we have the effective potential of the KTN black hole, it is possible to calculate the grey-body factors without solving the radial part of the Klein-Gordon equation (2.22), as we discussed in the previous section.

In order to apply Eq. (2.39), let us to return from the tortoise coordinate to the original coordinate. So that, the

effective potential (3.14) will be given in the following form:

$$V_{\omega\ell m}(r) = \frac{2 a m \omega}{\Delta} - \frac{a^2 m^2 - \ell(\ell + 1)\Delta}{\Delta(a^2 + l^2 + r^2)} - \frac{r - (2r^2 - 2Mr) - \Delta}{(a^2 + l^2 + r^2)^2} - \frac{2\Delta r^2}{(a^2 + l^2 + r^2)^3}. \quad (3.21)$$

Now, using Eq. (2.39), we have the following expression

$$\gamma_{\ell m}(\omega) \geq \text{sech}^2 \left[\frac{1}{2\omega} \int_{r_h}^{\infty} V_{\omega\ell m}(r) dr \right]. \quad (3.22)$$

Now solving the integral part of Eq. 3.22 (for instance for using Wolfram Mathematica[®]), we arrive at

$$\frac{1}{2\omega} \int_{r_h}^{\infty} V_{\omega\ell m}(r) dr = \frac{1}{8\omega(M^2(a^2 + l^2) + l^4)} (P_{\ell m} + Q_m(\omega) - R + S_m(\omega) + T_m), \quad (3.23)$$

where the functions $P_{\ell m}$, $Q_m(\omega)$, R , $S_m(\omega)$, and T_m were used in order to simplify the result of the integration and they are given by the following expressions[‡]:

$$P_{\ell m} = \frac{1}{(a^2 + l^2)^{3/2}} \left[\pi - 2 \arctan \left(\frac{r_h}{\sqrt{a^2 + l^2}} \right) \right] \\ \times \left[a^4 l^2 m^2 + M^2(a^2 + l^2) \left[2a^2(\ell^2 + \ell + 1) + (2\ell(\ell + 1) + 1)l^2 \right] \right. \\ \left. + a^2 l^4 (2\ell(\ell + 1) + m^2 + 2) + (2\ell(\ell + 1) + 1)l^6 \right], \quad (3.24)$$

$$Q_m(\omega) = \sqrt{\frac{1}{a^2 - l^2 - M^2}} am\pi \left[4\omega(M^2(a^2 + l^2) + l^4) - am(l^2 + M^2) \right], \quad (3.25)$$

$$R = \frac{2 \left[M^2(a^2 + l^2) + l^4 \right] \left[(2M + 1)(a^2 + l^2)^2 + r_h^2(a^2 + l^2) - 3l^2 r_h(a^2 + l^2) - l^2 r_h^3 \right]}{(a^2 + l^2)(a^2 + l^2 + r_h^2)^2}, \quad (3.26)$$

$$S_{m\omega} = \frac{2am \left[4\omega(M^2(a^2 + l^2) + l^4) - am(l^2 + M^2) \right] \arctan \left(\frac{M - r_h}{\sqrt{a^2 - l^2 - M^2}} \right)}{\sqrt{a^2 - l^2 - M^2}}, \quad (3.27)$$

$$T_m = a^2 m^2 M \left[\log(a^2 + l^2 + r_h^2) - \log(a^2 - l^2 - 2Mr_h + r_h^2) \right]. \quad (3.28)$$

Therefore using the result (3.23), we can have the expression for the greybody factor for a KTN black hole, which is given as follows:

$$\gamma_{\ell m}(\omega) \geq \text{sech}^2 \left[\frac{1}{8\omega(M^2(a^2 + l^2) + l^4)} (P_{\ell m} + Q_m(\omega) - R + S_m(\omega) + T_m) \right]. \quad (3.29)$$

After, analyzing Eq. (3.29) it is possible to identify that the only allowed value for m is zero, otherwise the expression (3.29) is indeterminate. Physically, when $m = 0$ means that the perturbations waves (bosons) of the field are directed to the central axis of rotation of the black hole. Thus, the field, is dominated only for axisymmetric perturbations⁸⁴.

[‡] ω , ℓ , and m have nature presented in section 2.2

Taking into account the previous consideration for the value of m , the greybody factor (3.29) does not depend on the functions that depend on m . Therefore, Eq. (3.29) can be expressed as follows

$$\gamma_{\ell 0}(\omega) \geq \text{sech}^2 \left[\frac{1}{8\omega (M^2 (a^2 + l^2) + l^4)} (P_{\ell 0} - R) \right]. \quad (3.30)$$

where R is given by equation (3.26) and $P_{\ell 0}$ as:

$$\begin{aligned} P_{\ell 0} = & \frac{1}{(a^2 + l^2)^{3/2}} \left[\pi - 2 \arctan \left(\frac{r_h}{\sqrt{a^2 + l^2}} \right) \right] \\ & \times \left[M^2 (a^2 + l^2) \left[2a^2 (\ell^2 + \ell + 1) + (2\ell(\ell + 1) + 1) l^2 \right] \right. \\ & \left. + a^2 l^4 (2\ell(\ell + 1) + 2) + (2\ell(\ell + 1) + 1) l^6 \right]. \end{aligned} \quad (3.31)$$

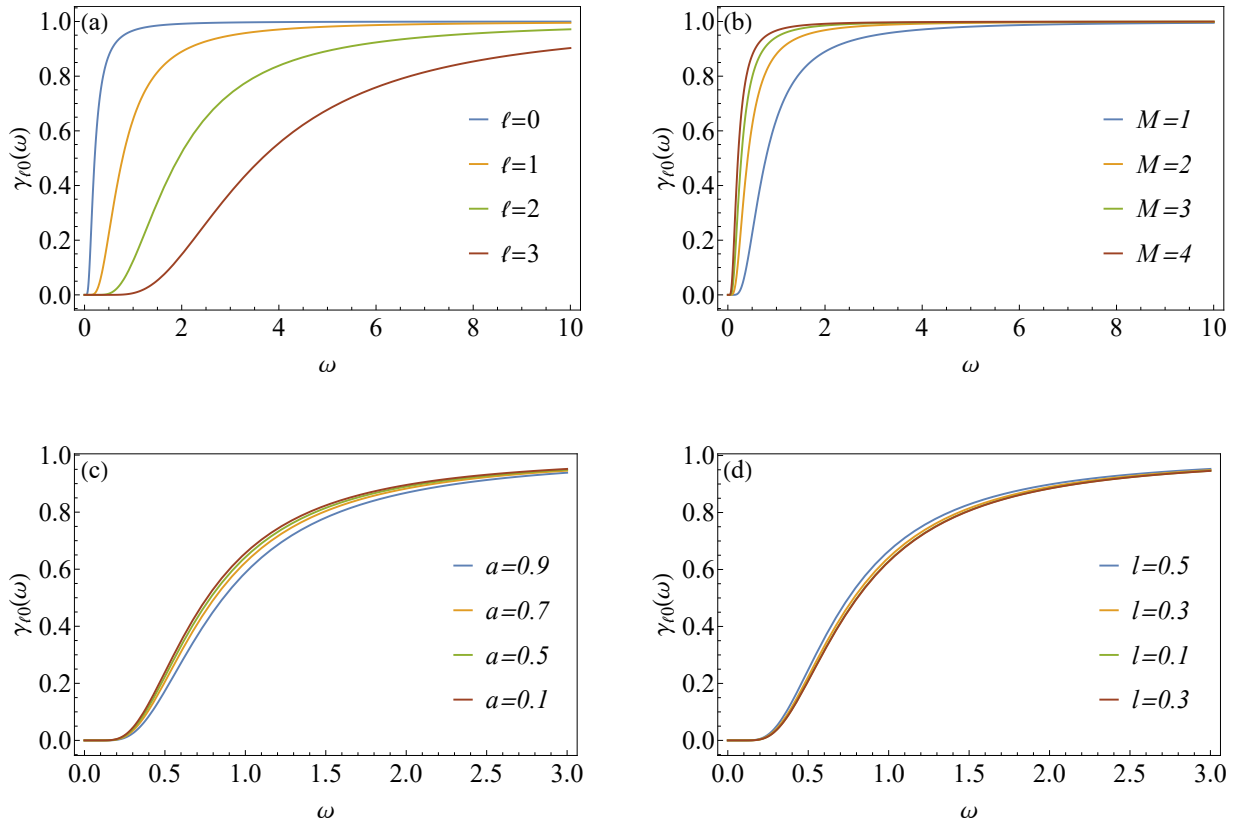


Figure 3.5: Plots of the greybody factors $\gamma_{\ell 0}(\omega)$ (3.14) for various situations. (a) $M = 1, a = 0.5, l = 0.3$, (b) $\ell = 1, a = 0.5, l = 0.3$, (c) $M = 1, \ell = 1, l = 0.3$, (d) $M = 1, \ell = 1, a = 0.5$ (M, a, l are in solar masses)

From figure 3.5, it is possible to analyze the behavior of the greybody factors for a KTN black hole. First of all, considering the change of the spheroidal harmonic quantum number ℓ in Fig. 3.5 (a), it is clear that increasing ℓ makes $\gamma_{\ell 0}(\omega)$ decrease. It means that a high value of bosonic radiation will reach an observer at infinity because the black hole absorbs fewer particles than the particles that escape from the black hole. In other words, when the ℓ number increases, the massless scalar field will oscillate more quickly and decay fast⁸⁵. Additionally, it is essential to mention that when the quantum number ℓ increases, the perturbation needs less frequency to escape from the potential (3.14). So, when ℓ is small, the oscillations of the perturbations are slow and decay for a longer time, which means that Hawking radiation is small compared to the other situation.

Looking at Fig. 3.5 (b), it is possible to see that the GFs are affected by the black hole mass. Massive black holes create fewer perturbations of the field that will escape from the hole's potential than low-mass black holes. As we discussed before, the less massive BHs have higher temperatures, and the GFs support it because the particles' emission is significant, which guarantees the perturbations will cross the potential barrier. In the other case, when the BHs are massive, their temperature is small because there is not much concentration of particles near the horizon; they escape from the potential. In other words, the mass allows us to measure the density of perturbations near the black hole horizon, which has a representative affections on the temperature of BHs.

Now, if we analyze the effect of the rotation parameter in the GFs Fig. 3.5 (c), it is possible to identify that the GFs tend to be similar. In general, there is no affection of the rotation parameter in the GFs, which means that despite the Kerr nature of the BH, the amount of radiation that comes away from the regions near the event horizon is approximately the same for all rotations. There is a small difference for low frequencies of the spin-0 particles. In the same way, considering the change in the nut parameter Fig. 3.5 (d), there is no effect in the GFs, which is an interesting behavior as we expected to have a real variations in the GFs as a consequence of the nut charge.

Additionally, the nature of the perturbations has a tangible impact on the greybody factors. If we have perturbations with small oscillations, the GFs indicate low emission of Hawking radiation; otherwise, if we have a high oscillating system (high values of ℓ), it is possible to have a high amount of radiation reaching an observer or detector. Moreover, considering the change in mass, it was possible to identify the relation of the GFs with the temperature of the black hole. Finally, the rotation and different nut parameters do not affect the tunneling of the particles through the potential barrier generated by the black hole.

3.3.2 Emission Rates

As we discussed, not all positive-energy particles or massless scalar perturbations can leave the black hole. Some of them suffer a reflection in the black hole due to the potential barrier surrounding it. Therefore, the grey-body factors will affect the energy emission rate. A low value in the GFs indicates that the fraction of particles that escape from the potential barrier generated by the BH is high. Therefore, GFs are a good indicator of the amount of Hawking radiation that reaches infinity.

When studying the Hawking radiation emitted by black holes, we will consider the assumption that the black hole is in a state of thermal equilibrium with its surroundings. Expressly, we assume that the temperature of the black hole remains constant between the emissions of two consecutive particles^{85,86}. This assumption leads us to

model the system using the canonical ensemble. Additionally, we consider that the emission is dominated by the mass, thus, formula (2.41) will work without problems.

In the same way, Hawking radiation is an essential quantum feature that carries information about the dynamics of the black hole evaporation. Therefore, the energy emission rate of the black hole will depend on the parameters that describe the black hole. In that case, the dynamics of the mass, angular momentum, and nut parameter are essential to understand the Hawking radiation for the KTN black hole. To carry out our analysis, we will consider the model that Kokkotas et.al⁸⁷ and Eq. (2.42), which allow us to describe the emission rates for mass, angular momentum, and nut parameter. Additionally, we are going to use values of $\ell \leq 3$, as these values guarantee a real contribution to the radiation that is emitted by the black hole⁸². In the same way, we are going to take m to evolve from 0 to the maximum value of ℓ . So that, $0 \leq \ell \leq 3$ and $0 \leq m \leq 3$.

Moreover, it is essential to analyze the behavior of angular momentum concerning the energy at infinity, where the wave is composed of many quanta, each of them with energy $E = \omega$ and angular momentum in the φ direction $J = m$. Thus, the ratio of the total angular momentum to the total energy carried by the wave across a hypothetical sphere must be $\frac{m}{\omega}$ ⁸⁸.

Emission Rate for Energy

From Eq.(2.41), it is possible to see that the emission rates are proportional to the greybody factors. Thus, the energy emission rate is given as follows

$$-\frac{dM}{dt} = \sum_{\ell=0}^3 \sum_{m=0}^3 \gamma_{\ell 0}(\omega) \frac{\omega}{\exp(\omega/T_H) - 1} \frac{d\omega}{2\pi}. \quad (3.32)$$

From figure 3.6, it is possible to see that the emission rate changes depending on the black hole mass. First, the emission for massive black holes is very weak compared to less massive black holes. It means more particles are emitted during radiation when the BHs are less massive. If we see the GFs for changes in mass, figure 3.5 (b), the deviation of standard Hawking radiation[†] is greater for massive black holes compared to less massive ones, which reinforce the description above. The potential of less massive black holes is weak, so the amount of particles captured by the black hole is small. It means we will have more radiation moderated by the GFs that reach an asymptotic observer. On the other hand, the massive BHs have a strong potential, meaning more particles will not escape from the hole. Therefore, the amount of particles that will reach infinity as radiation is slight.

In the same way, considering the black hole temperature, it is possible to say that it agrees with the previous results. The temperature and the emission rate have a direct proportionality.

Emission Rate for Angular Momentum

Taking into account Eq. (2.41) and the ratio of angular momentum respect to the energy at infinity m/ω , the emission rate is defined as follows

$$-\frac{dJ}{dt} = \sum_{\ell=0}^3 \sum_{m=0}^3 \int \gamma_{\ell 0}(\omega) \frac{m}{\exp(\omega/T_H) - 1} \frac{d\omega}{2\pi}. \quad (3.33)$$

[†]"standar" refers to a pure blackbody radiation.

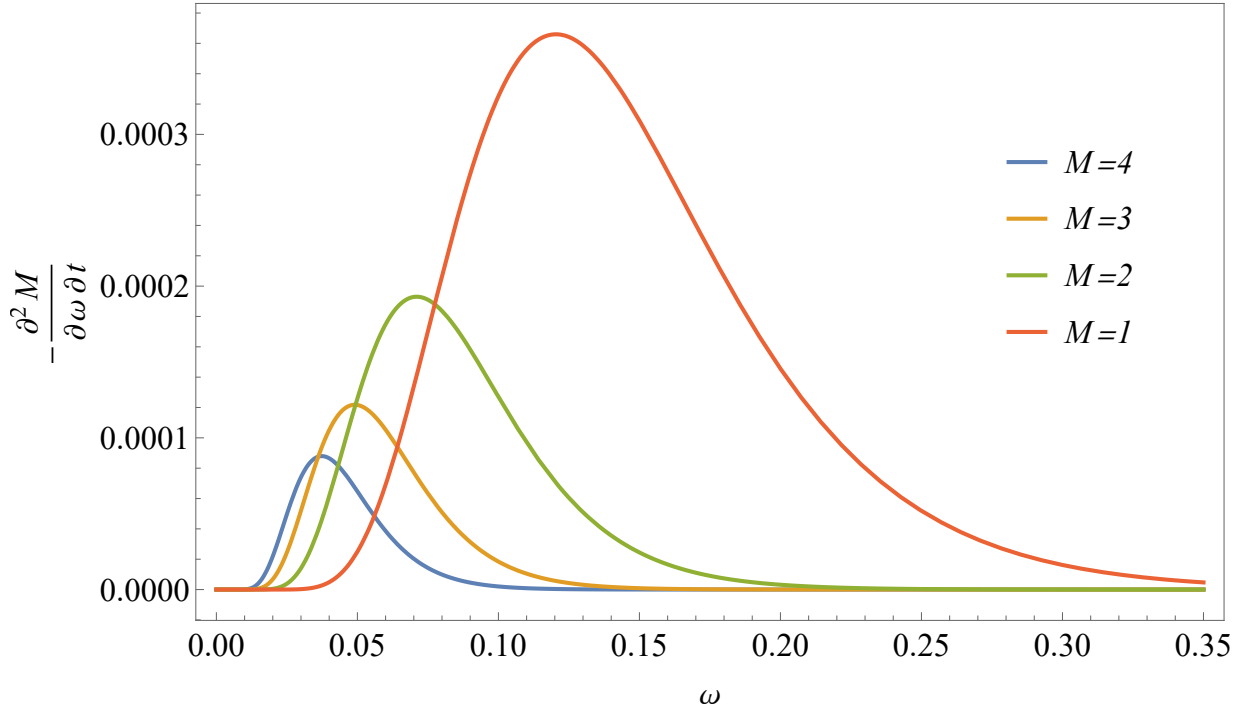


Figure 3.6: Energy emission rate for KTN black hole for different masses M . We set the parameters $a = 0.7$, $l = 0.3$. (M , a , l are in solar masses)

From the data in Figure 3.7, noticeable variations in the angular momentum emission rate become apparent with rotation changes. In essence, this indicates that particles are extracting energy from the rotation of the black hole, a phenomenon recognized as super-radiance⁸⁸. This occurs when $\omega < m \Omega_{KTN}$. This condition is satisfied in the majority of cases. Emission rates are higher for smaller rotations than higher rotations, where the rate tends to diminish. The primary reason is that particles find it challenging to escape as a black hole approaches its maximum rotation due to the significant dragging effect, causing them to rotate with the BH. Conversely, the dragging effect diminishes when the hole's rotation decreases, allowing particles to escape more easily from the event horizon. Thus, the level of rotation acts as a barrier, impeding particles from reaching infinity as Hawking radiation.

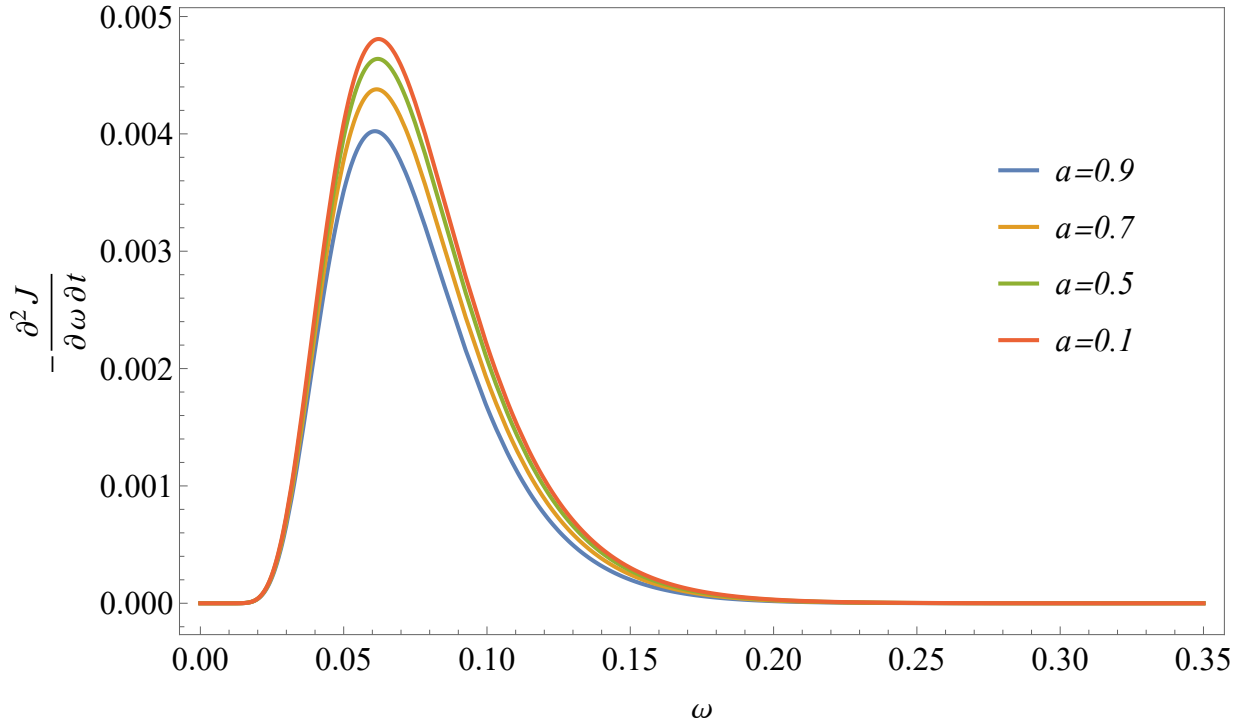


Figure 3.7: Angular momentum emission rate for KTN black hole for different rotation parameters a . We set the parameters $M = 2$, $l = 0.3$. (M, a, l are in solar masses)

Emission Rate for the Nut Parameter

Based on the model of Kokkotas et al.⁸⁷, we will assume a fundamental quantity n that characterizes the nut parameter. This quantity will be entirely theoretical because there are no measurements of the parameter l . In general, let us assume that at infinity, a wave carries information about the nut parameter, which is quantized. Therefore, the total nut parameter l is defined as $l = n$. Analyzing the ratio of the total nut parameter to the total energy carried by the wave across a hypothetical sphere must be $\frac{n}{\omega}$.

Based on that, the evolution of the nut parameter will be defined as follows.

$$-\frac{dl}{dt} = \sum_{\ell=0}^3 \sum_{m=0}^3 \int \gamma_{\ell 0}(\omega) \frac{n}{\exp(\omega/T_H) - 1} \frac{d\omega}{2\pi}. \quad (3.34)$$

In figure 3.8, it is possible to see that there is approximately no change in the emission due to the change of the nut parameter. It means that waves will extract the nut parameter at the same rate despite its different values.

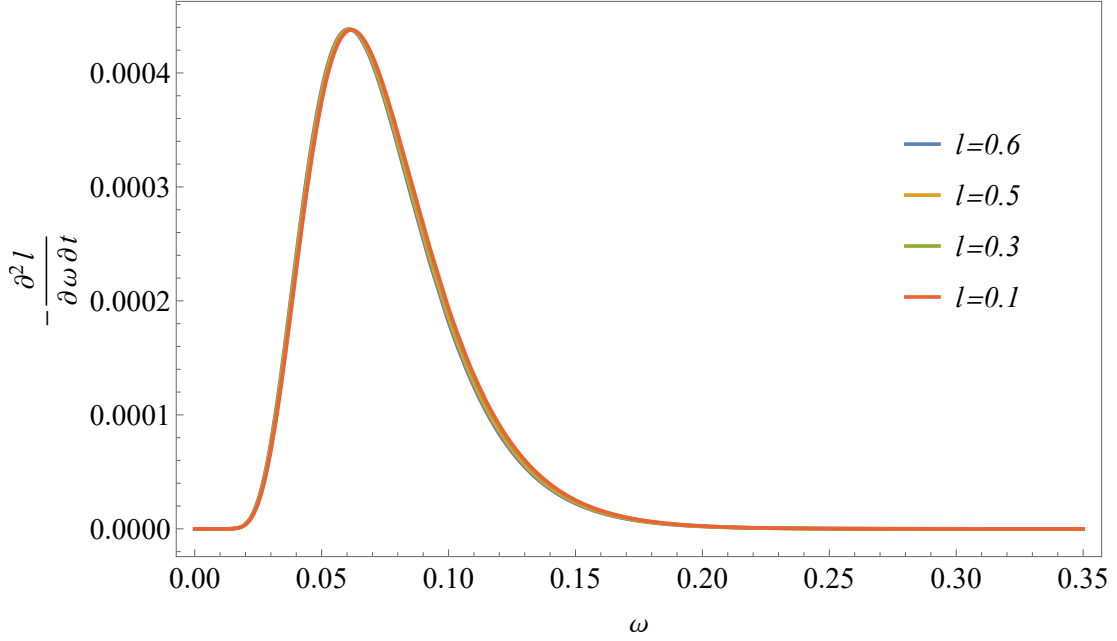


Figure 3.8: Nut parameter emission rate for KTN black hole for different nut parameters l . We set the parameters $M = 2$, $a = 0.7$, and $n = 0.15$ (M , a , l are in solar masses. n is dimensionless).

3.4 Differential decays.

The differential decay practically quantifies the rate of the emission of a specific quantity^{||}; in that case the emission of mass, angular momentum and nut parameter.

From table 3.2, it is possible to see that the differential decay for the mass is minor compared to the other decays, which means that the emission process for the mass is slow. In general, the evaporation for a KTN black hole is given by the following relation;

$$-\frac{dJ}{dt} > -\frac{dl}{dt} > -\frac{dM}{dt}. \quad (3.35)$$

Based on relation (3.35), a Kerr-Taub-Nut black hole will first lose the angular momentum, then the nut charge, and finally the mass. In other words, if we want to study a KTN black hole during different periods, it could be possible to neglect some parameters. For example, in our case, we can neglect the angular momentum and study a Taub-Nut black hole. From another point of view, after the angular momentum, we can avoid the nut charge, which means that we are analyzing a Schwarzschild black hole. One example of this simplification was made by Page, where he neglected the charge of the black hole and considered only a Kerr black hole⁷⁶.

^{||}The results were obtained integrating the data from the emission rates plots

Table 3.2: Differential decays for the mass, angular momentum and nut parameter. The fundamental nut parameter is defined as $n = 0.15$.

Mass $M [M_\odot]$	Rot. parameter $a [M_\odot]$	nut charge $l [M_\odot]$	$-\frac{dM}{dt} = \alpha_1$	$-\frac{dJ}{dt} = \alpha_2$	$-\frac{dl}{dt} = \alpha_3$
1	0.2	0.10	8.9×10^{-5}	9.3×10^{-4}	9.3×10^{-5}
2	0.3	0.20	1.6×10^{-5}	3.1×10^{-4}	3.1×10^{-5}
3	0.4	0.30	6.2×10^{-6}	1.8×10^{-4}	1.8×10^{-5}
4	0.5	0.35	3.3×10^{-6}	1.2×10^{-4}	1.2×10^{-5}
5	0.6	0.40	2.1×10^{-6}	9.6×10^{-5}	9.6×10^{-6}
6	0.7	0.50	1.4×10^{-6}	7.8×10^{-5}	7.8×10^{-6}

3.5 The Page Curve for a Kerr-Taub-Nut Black Hole

Hitherto, we have developed the main ingredients in order to calculate the time dependence of the Hawking radiation entropy, which is an alternative to solve the information loss paradox.

3.5.1 Time dependence of the Kerr-Taub-Nut black hole

The first step to calculate the entanglement entropy (see table 2.4.2) considering the black hole and its radiation as a quantum system is to look for the time evolution of the parameters that describe the black hole. In this case, the mass, angular momentum, and nut parameter (see appendix C for more details).

First of all, let us consider the model (2.49) and apply it to the KTN black hole parameters.

For the mass;

$$\frac{dM(t)}{dt} = -\frac{\alpha_1}{M(t)^2}. \quad (3.36)$$

For the angular momentum;

$$\frac{dJ(t)}{dt} = -\frac{\alpha_2 a_*}{M(t)}, \quad (3.37)$$

where $a_* = \frac{J}{M^2}$. For the nut charge, it is important to consider that we need to modify the model (2.49)

$$\frac{dl(t)}{dt} = -\frac{\alpha_3 l_*}{M(t)}, \quad (3.38)$$

where $l_* = \frac{l}{M}$ is the dimensionless nut parameter.

The $\alpha_1, \alpha_2, \alpha_3$ come from the differential decays for every parameter of the black hole.

Combining equations (3.36), (3.37), and (3.38) it is possible to have a system of differential equations. Additionally, in order to make the solution easy, let us consider that the parameters l_* and a_* as independent variables⁷⁶ and set them based on the initial conditions of the problem implying that $a_* = \frac{J_0}{M_0^2}$ and $l_* = \frac{l_0}{M_0}$.

Therefore, the solutions are given by the following expressions: For mass;

$$M(t) = (-3\alpha_1 t + c_1)^{1/3}. \quad (3.39)$$

Now, taking into account that at $t = 0$ we have an initial mass M_0 and that at the final step of the evaporation $M = 0$, we have the following results;

$$M(t) = (-3\alpha_1 t + M_0^3)^{1/3}, \quad (3.40)$$

where the total time of decay is expressed as follows;

$$t_{decay} = \frac{M_0^3}{3\alpha_1}, \quad (3.41)$$

which describes the lifetime of the black hole. Additionally, it is clearly to see that t_{decay} is proportional to the initial mass of the black hole and inversely proportional to the rate of emission or differential decay. It means that, if the differential decay is small, the time will be very large, otherwise, the time will be small.

Therefore, the final expression for Eq. (3.39) is

$$M(t) = M_0 \left(1 - \frac{t}{t_{decay}}\right)^{1/3}. \quad (3.42)$$

As we did for the mass case, the initial and final conditions for the nut parameter and angular momentum must be considered to obtain an expression for each time decay and expressions that give the time evolution for the angular momentum and nut parameter in terms of their initial value. Therefore;

For angular momentum;

$$J(t) = J_0 - \frac{\alpha_2 a_* M_0^2}{2\alpha_1} \left[1 - \left(1 - \frac{t}{t_{decay}}\right)^{2/3}\right], \quad (3.43)$$

where the time that angular momentum takes to decay is

$$t_{moment} = 1 - \left(\frac{\alpha_2 a_* M_0^2 - 2\alpha_1 J_0}{\alpha_2 a_* M_0^2}\right)^{3/2} t_{decay}. \quad (3.44)$$

For the nut parameter;

$$l(t) = l_0 - \frac{\alpha_3 l_* M_0^2}{2\alpha_1} \left[1 - \left(1 - \frac{t}{t_{decay}}\right)^{2/3}\right], \quad (3.45)$$

where the time that the nut charge takes to decay is

$$t_{nut} = 1 - \left(\frac{\alpha_3 l_* M_0^2 - 2\alpha_1 L_0}{\alpha_3 l_* M_0^2}\right)^{3/2} t_{decay}. \quad (3.46)$$

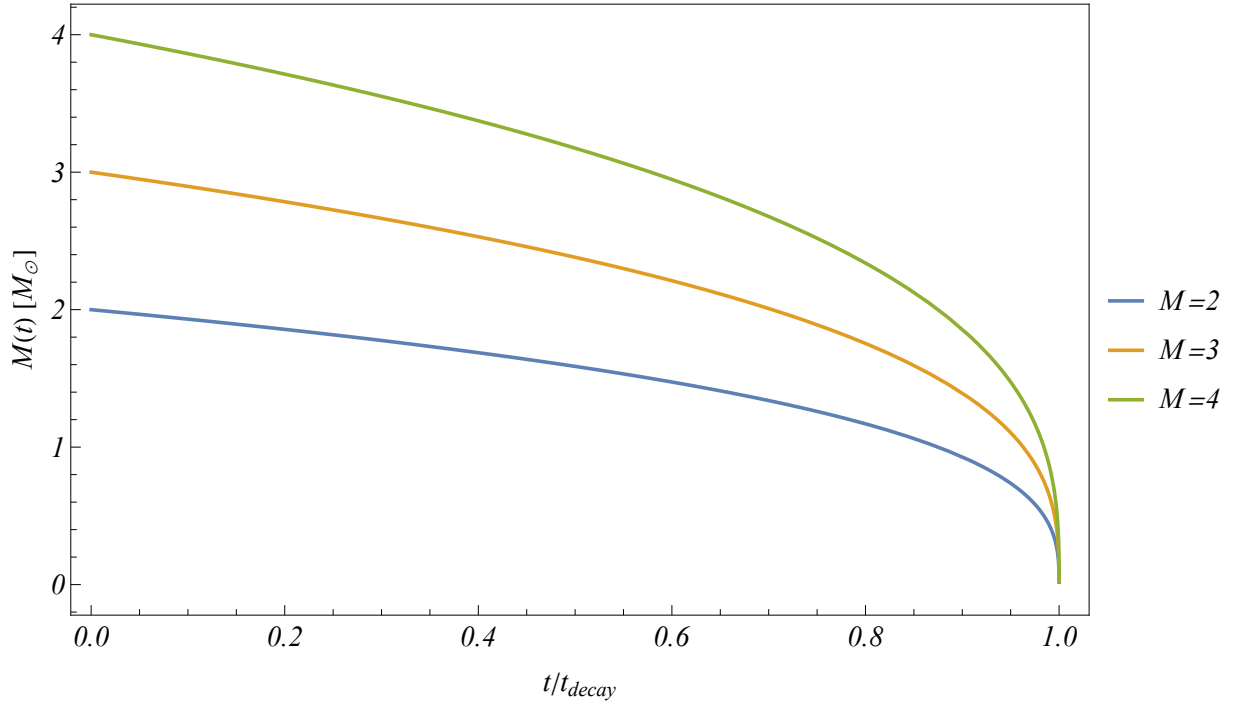


Figure 3.9: Mass-time dependence profiles for different black hole masses (in solar masses).

From figure 3.9, it is possible to identify that black hole masses evolve differently depending on the initial mass. The massive BHs evolve more slowly than the less massive black holes makes sense because, as we discussed, the KTN black holes with small masses emit more radiation than the others, and as a consequence of this, the black hole will lose mass much faster than the massive ones.

Additionally, it is possible to get the same conclusion if we analyze the time of decay. Using the formula (3.41), we have the following results:

Table 3.3: Lifetime for different KTN black hole masses.

Mass $M [M_{\odot}]$	α_1	t_{decay}/M_{\odot}^3
1	8.9×10^{-5}	3.8×10^3
2	1.6×10^{-5}	8.5×10^4
3	6.2×10^{-6}	4.8×10^5
4	3.3×10^{-6}	1.6×10^6

Looking, the data from table 3.3, it is possible to confirm that massive black holes practically have a lifetime that is very long in comparison with the less massive black holes.

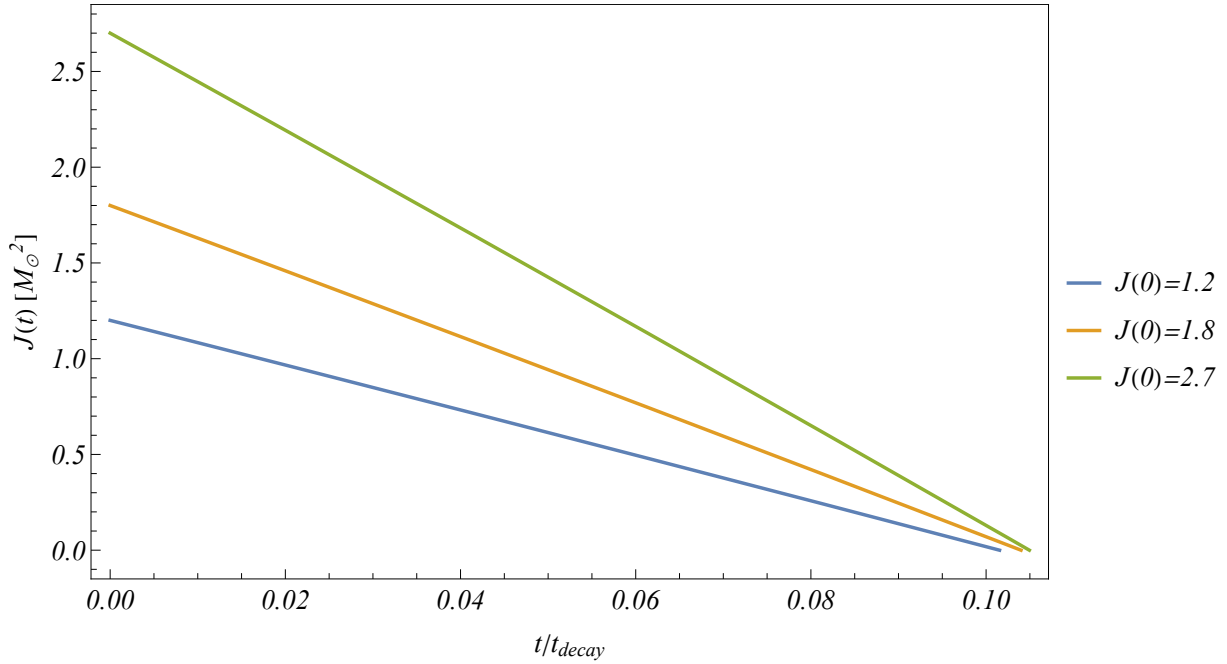


Figure 3.10: Angular momentum-time dependence profiles for different black hole initial angular momentum. The physical parameters are $M = 3 M_{\odot}$ and $l = 0.3 M_{\odot}$

Now, analyzing the evolution of the angular momentum 3.10, it is possible to describe the following aspects. Firstly, the evolution of the angular momentum happens approximately linearly. In the same way, when we have small rotations, the angular momentum stays for less time; instead, when we increase the rotation, angular momentum vanishes slowly. Physically, it means that when a black hole rotates slowly, the particles that escape from the event horizon regions extract rotational energy. As the rotation is slight, the black hole's angular momentum vanishes faster than when the rotations are high. As we discussed, it takes a lot of time to happen. In general, it means that when the rotation increases, it contributes slightly to the energy emission, and practically, depending on the amount of rotation, the angular momentum will eventually disappear.

Note that analyzing the nut parameter evolution (Fig. 3.11) is similar to the angular momentum evolution. For small nut values, the time it takes the nut parameter to decay is less extended than in cases with high nut parameters. In general, as in the case of angular momentum, the presence of nut parameters affects its evolution. Physically, it implies that particles extract energy from the nut parameter, which happens fast when it is small.

Now, comparing the evolution of angular momentum (3.10) and nut parameter (3.11), it is noticeable that the angular momentum has a shorter lifetime than the nut parameter. This suggests that the percentage of the contribution of angular momentum to the energy emission is much more significant than the contribution of the nut parameter, allowing a fast decay of the angular momentum.

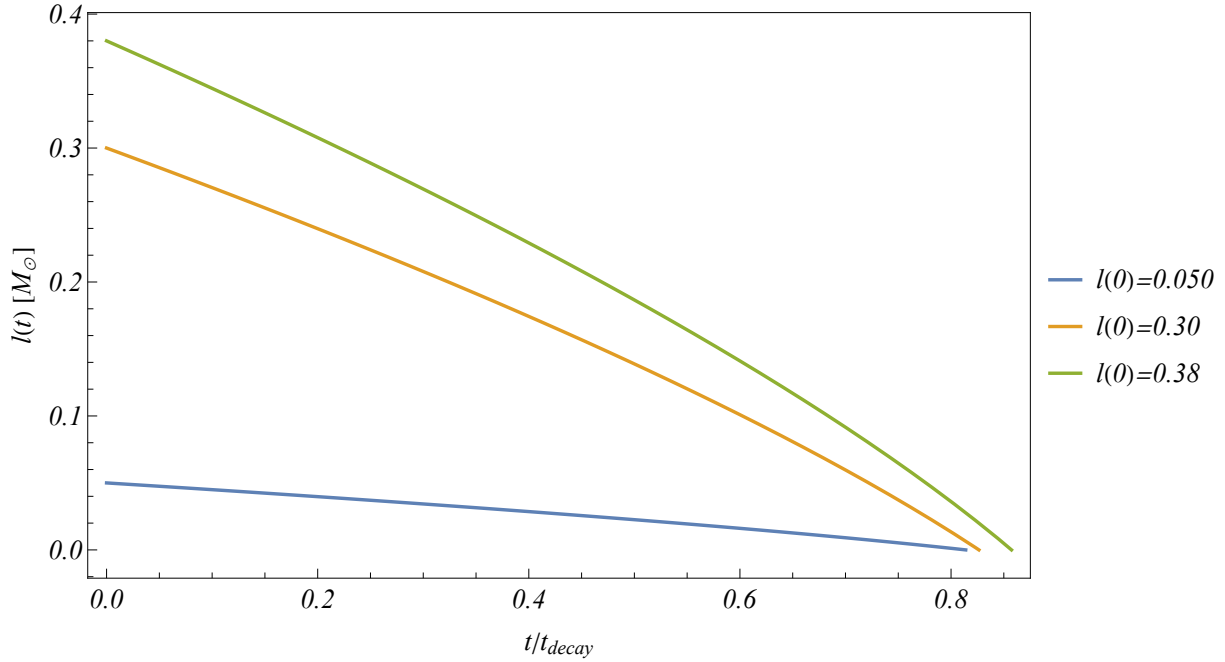


Figure 3.11: Nut parameter time dependence profiles for different initial nut values. The parameters are $M = 3 M_{\odot}$ and $a = 0.4 M_{\odot}$ (l is in solar masses).

3.5.2 The Von Neumann Entropy

Now, once we have the evolution of the parameters for a KTN black hole. It is possible to calculate the evolution of the Bekenstein-Hawking entropy.

Let us to replace the equations (3.39), (3.43), and (3.45) into expression (3.7), then we have

$$S_{BH}(t) = 2\pi \left[M(t)^2 + L(t)^2 + M(t) \sqrt{M(t)^2 + L(t)^2 - \frac{J(t)^2}{M(t)^2}} \right]. \quad (3.47)$$

In figure 3.12, the time dependence of the Bekenstein-Hawking entropy for a KTN black hole is presented. As we discussed, this entropy states that the black hole entropy is proportional to its event horizon (see subsection 2.3.1). Since the black hole is losing energy while emitting radiation, it losses mass and shrinks until it is completely evaporated. Hence, this entropy begins at some positive value and it decreases to zero⁵.

On the other hand, based on the the work of Nian¹⁷ and Page¹⁶ the entropy of the radiation is given by the following expression:

$$S_{rad} = \beta (S_{BH}(0) - S_{BH}(t)), \quad (3.48)$$

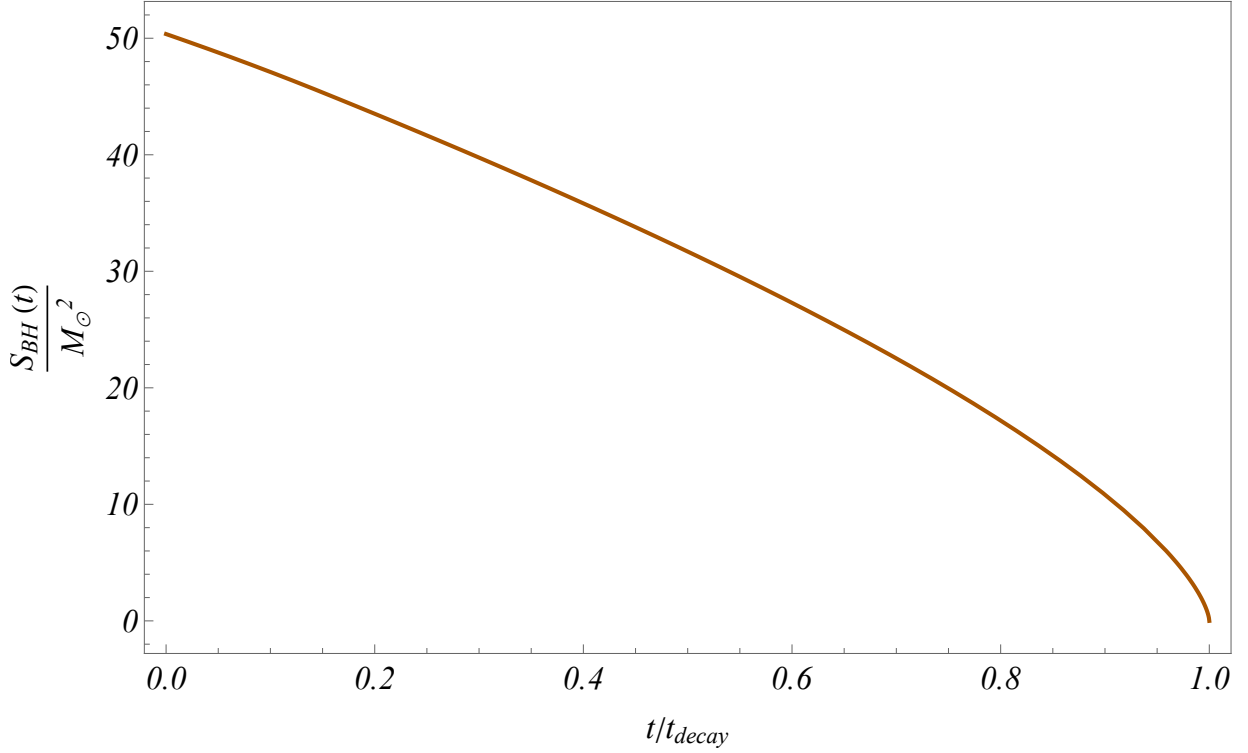


Figure 3.12: Bekenstein-Hawking entropy evolution $S_{BH}(t)$ for a Kerr-Taub-Nut black hole. The physical parameters are: $M(0) = 2$, $J(0) = 0.6$, $l(0) = 0.2$ (M and l in solar masses. J in M_{\odot}^2).

where β is a parameter that characterizes the fact that the entropy of the Hawking radiation is greater than the coarse-grained entropy of the black hole. We will use the value that Page calculated as a fact that the final evaporation state of the black hole can be approximately as a Schwarzschild black hole emitting photons⁸⁹. Therefore β is expressed as follows

$$\beta = \frac{\frac{dS_{rad}}{dt}}{-\frac{dS_{BH}}{dt}} \approx 1.5003. \quad (3.49)$$

The value of (3.49) suggests that the radiation entropy would be 1.5003 times that by which the BH decreased. The previous value comes from the numerical calculations of change of entropy of radiation and Bekenstein-Hawking entropy, under the assumption that the black hole is only emitting photons^{16,89}. In general, the calculations of β is an active area of work¹⁶. In that sense we are going to use different values of it in order to see the effect in the radiation entropy and Von Neumann entropy.

In order to have the expression for the entropy of the Hawking radiation (3.48), it is only necessary to use the expression for the Bekenstein-Hawking entropy (2.31) and evaluate it at time $t = 0$ and at time t . After that, we can

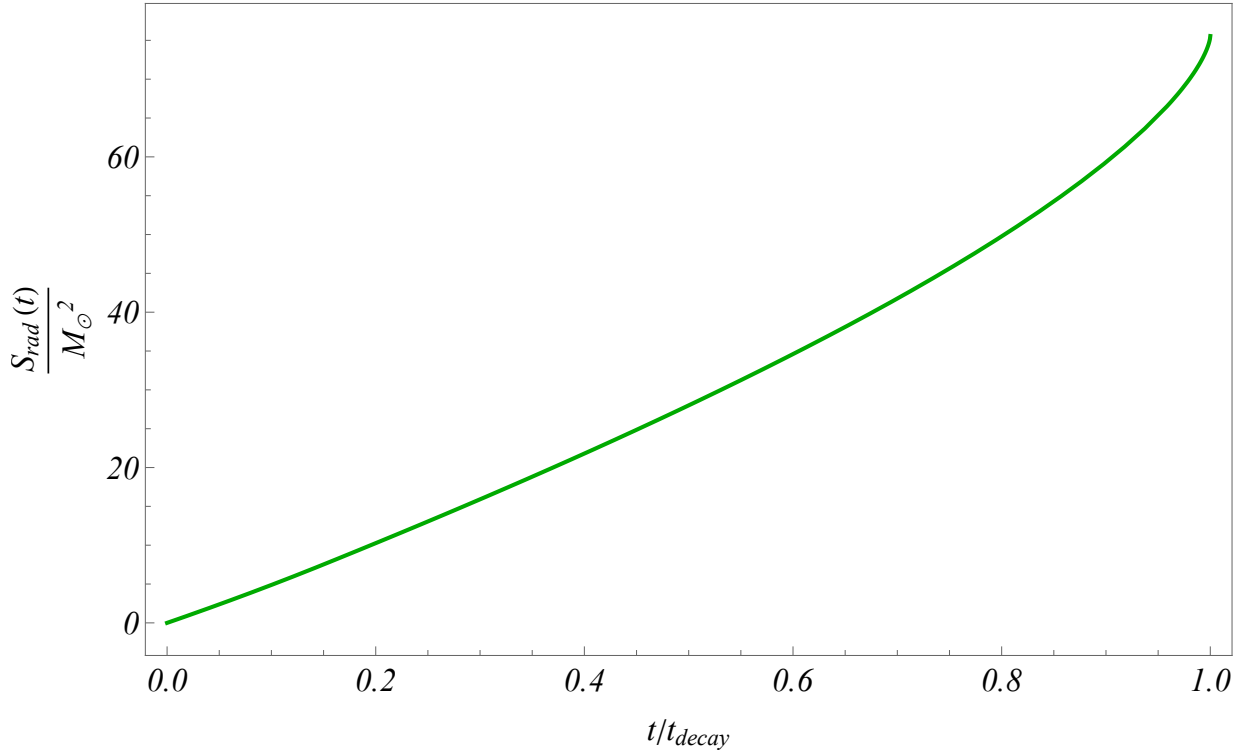


Figure 3.13: Entropy of Hawking radiation evolution $S_{BH}(t)$ for a Kerr-Taub-Nut black hole. The physical parameters are: $M(0) = 2$, $J(0) = 0.6$, $l(0) = 0.2$ (M and l in solar masses. J in M_{\odot}^2).

use these results in equation (3.48). The calculations could be done manually or in some mathematical software like Mathematica (see appendix D). In figure 3.13, we plot the entropy of the Hawking radiation for a KTN black hole with mass $M = 2$, angular momentum $J = 0.6$, and nut parameter $l = 0.2$. The physical interpretation is that just after the formation of the black hole, the entropy of the radiation is zero since there is no radiation yet. Afterwards, the entropy increases as the Hawking radiation is emitted until the black hole evaporates completely^{3,5,55}.

Now comparing the the curves 3.12 and 3.13 one problem is noticeable. Since one curve increases and the other decreases, they will met at some time; therefore, the entropy of the radiation becomes higher than the thermodynamic entropy of the black hole, and the inequality (2.48) will not longer be valid.

As we discussed in section 2.4, it is necessary to calculate the entanglement entropy between the black hole and its radiation since both form a single quantum system. Using the work made by Page¹⁶, the entanglement entropy (i.e., von Neumann entropy of the system) is given using the Heaviside step function because the Page time represents a threshold to put together the Bekenstein-Hawking and radiation entropies. Thus,

$$S_{VN}(t) = S_{rad} \theta(t_{page} - t) + S_{BH} \theta(t - t_{page}), \quad (3.50)$$

where t_{page} represents the time at which the thermodynamic entropy and the radiation entropy met. Therefore, in order to obtain it, the expressions (3.47) and (3.48) must be equalled and solved for time.

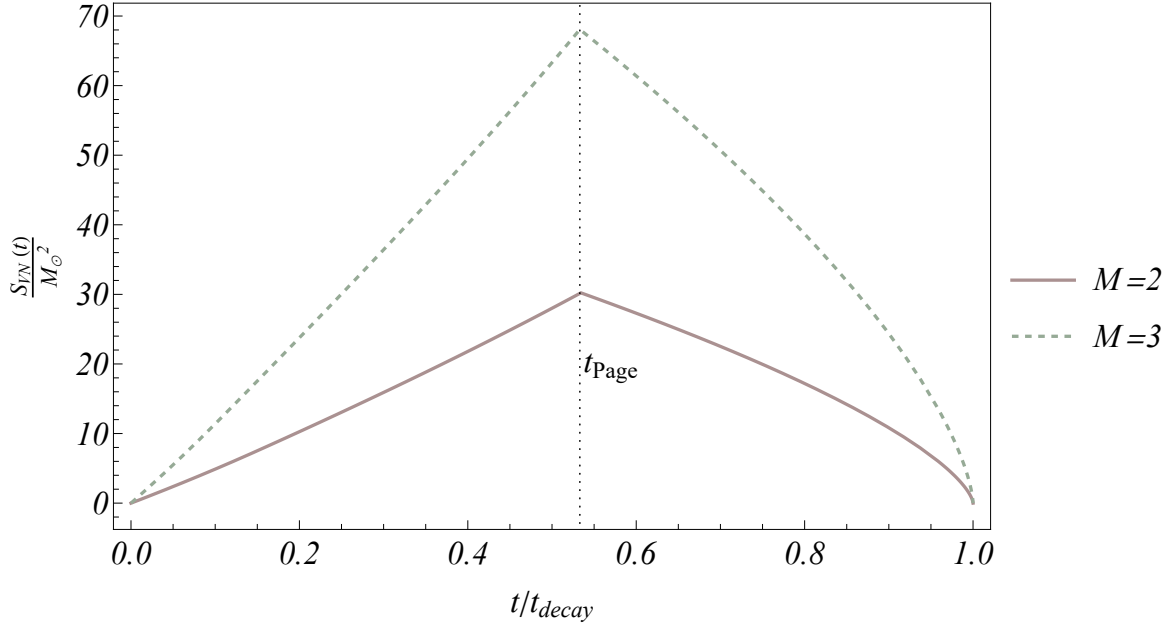


Figure 3.14: Von Neumann entropy evolution for an initially pure KTN black hole. $M = 2$, $J = 0.6$, $l = 0.2$ (thick line), $M = 3$, $J = 1.2$, $l = 0.3$ (dashed line), (M and l in solar masses. J in M_{\odot}^2).

From figure 3.14, it is possible to extract valuable information. Firstly, if a KTN black hole together with its radiation is considered as a pure quantum state, it means that there is a unitary mechanism that allows to conserve the information, as a pure state is evolving into a pure one. Moreover, as the Von Neumann entropy quantifies our lack of knowledge about a system, it is saying that at the end of the evaporation it is possible to have all knowledge about the black hole information. Additionally, considering the black holes parameters, it is clearly to see that when the mass, angular momentum, and nut parameter increase, it is more difficult to know the black hole information due to higher values in comparison when the parameters (i.e., mass, angular momentum, and nut parameter) are more small.

Furthermore, despite of the value of the black hole parameters, the time that takes the mass to be reduced to half is approximately the same⁷³. It is justified due to the Page time $t_{Page} = \frac{t}{t_{decay}}$ is similar for each situation; $t_{Page} = 0.534308$ for a mass $M = 2$, and $t_{Page} = 0.533057$ for a mass $M = 3$.

As we discussed previously, we will assume some values for the β parameter in order to see its implications on the Page curve. From figure 3.15, it is clear that when β is small it entails an increase in the Page time. It implies that the black hole radiation takes more time in order to reduce the black hole mass to the half. On the other hand, when the β parameter increases the Page time decreases. In general, it is possible to say that when the parameter is

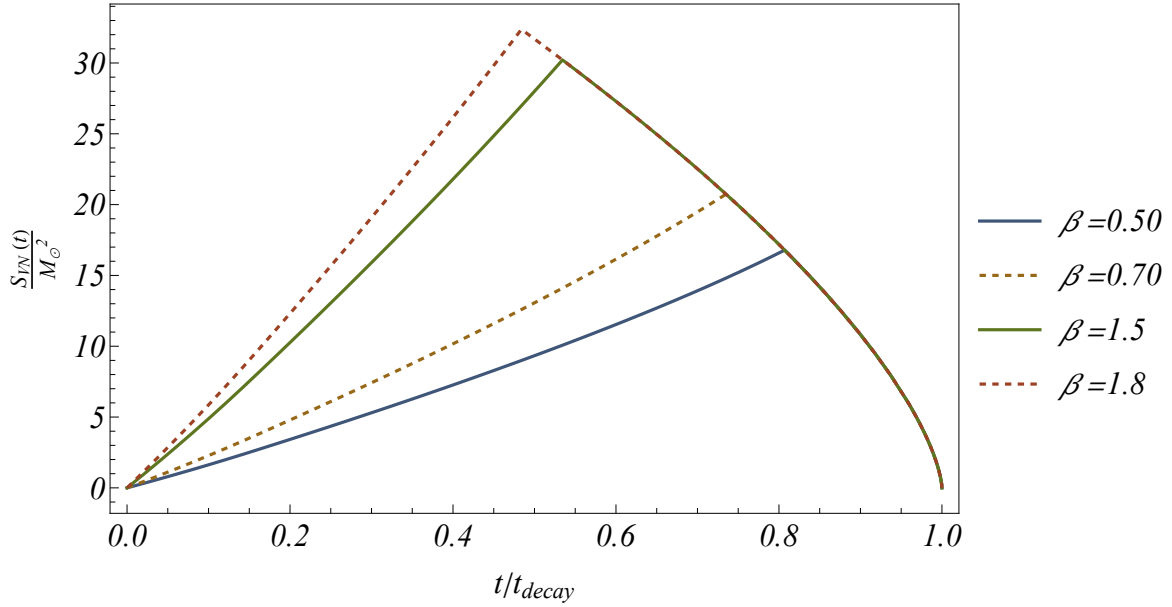


Figure 3.15: Von Neumann entropy evolution for an initially pure KTN black hole for different β values (see Eq. (3.49)). We set $M = 2$, $J = 0.6$, $l = 0.2$ (M and l in solar masses. J in M_{\odot}^2).

big, the process of evaporation is dominated by Hawking radiation. In other words the particle production is very high that the black hole evaporation process is not difficult. On the other side, small values implies that practically there is a lack of radiation that allows a slow evaporation of the black hole. The Page time for the different values of β are shown in table 3.4.

Table 3.4: Page time for an initially pure KTN black hole for different β values. $M = 2 M_{\odot}$, $J = 0.6 M_{\odot}^2$, $l = 0.2 M_{\odot}$

β	Page time	$\frac{t}{t_{\text{decay}}}$
0.50	8.1×10^{-1}	
0.70	7.4×10^{-1}	
1.5	5.3×10^{-1}	
1.8	4.8×10^{-1}	

Chapter 4

Conclusions and outlook

Throughout this research, we made different calculations to get the Page curve for a Kerr-Taub-Nut black hole. After solving the problem presented in the thesis, we briefly analyzed the space-times that contain a nut parameter (nut charge), including the Kerr-Taub-Nut space-time. Following the analysis, the first step was to calculate the temperature of the black hole given by Eq.(3.2). We identified that low-mass black holes have higher temperatures than massive black holes. Additionally, it is essential to mention that the temperature profile for a KTN black hole is very similar to that of a Kerr black hole. Considering all black hole masses, the value of the nut parameter affects the temperature. High nut values imply high temperatures. Instead, small values allow a Kerr-like temperature.

After that, we calculated the Bekenstein-Hawking entropy for a KTN black hole using Eq.(2.31) and compared it with the entropy of a rotating and non-rotating black hole. From these calculations, we could identify that the number of microstates for the black holes is similar, which means that it does not matter what type of black holes we are interested in studying; the level of complexity tends to be similar. Furthermore, considering the implications of the rotation for temperature, it was found that when the rotation increases, the temperature decreases.

In order to study Hawking radiation, we considered that the space-time surrounding the Kerr-Taub-Nut black hole is a massless scalar field. In order to study the perturbations that the black hole generates in this field, we analyzed the Klein-Gordon equation in a curved space (2.22) by using the radial part of the Teukolsky equation (3.9). We found that the effective potential that the black holes generate disappears at infinity due to its tendency to zero in the asymptotic limit. Moreover, an increase in the black hole rotation tends to make the potential broader and less intense. Likewise, the potential, specifically at the event horizon, is smaller for low-mass black holes than for massive ones.

From that result, we could go further into the analysis, and the greybody factors, which represent the probability of a particle being absorbed by the black hole, were calculated. From this, it was possible to determine that the probability tends to change depending on the level of the perturbations. For low-perturbed fields, the probability is more significant than for high-perturbed fields. Additionally, the changes in mass imply a modification of the probability. Lower masses represent less probability than the higher masses. In that sense, fewer particles will escape infinity in the second case. Less massive black holes possess a small effective potential, allowing more

particles to escape than in the massive black holes scenario. Thus, massive black holes have a higher probability of capturing particles. In the other case, small black holes have a lower probability of absorption, which guarantees a high number of particles that can reach infinity. Additionally, the rotation and nut parameters have approximately the same absorption probability, which feeds the idea that the nut parameter is a source of pure angular momentum.

In black hole evaporation, we computed emission rates for the parameters characterizing the Kerr-Taub-Nut black hole. Our analysis indicated that the emission of angular momentum diminishes faster than the nut charge and mass of the black hole, implying that the angular momentum's depletion precedes the other parameters. Eventually, during the final stages of evaporation, emissions align with those of a Schwarzschild black hole.

Finally, we used the model proposed by Page (2.49) to approximate the evolution of the KTN black hole parameters. We confirmed that the parameter's evolution agrees with the emission rates. After that, the models (3.42), (3.43), and (3.45) were used to see the evolution of the Bekenstein-Hawking and Hawking radiation entropy. We used the previous results to calculate the Von Neumann entropy that correlates the black hole and its radiation. We found that it follows the Page Curve, preserving the information during the evaporation of a Kerr-Taub-Nut black hole. Additionally, we showed that regardless of the black hole parameters, the KTN black holes lose half of their initial mass simultaneously. Moreover, we analyzed the effect of the β parameter, which quantifies the amount of Hawking radiation. The results suggested that for high values, the black holes lose half of their masses much faster than when the values are small.

In general, we described the Page curve for a Kerr-Taub-Nut black hole. This is an important goal because it suggests that there is a unitary mechanism that guarantees that quantum information is not lost. Additionally, we obtain the result under the assumption that the angular momentum dominates the emission; therefore, if the potential associated with the cosmic strings is included in the analysis, it is expected a change in the emission rates and, consequently, a change in the time evolution of the black hole parameters. In the same way, the β parameters showed that it is necessary to study the Page curve. Therefore, future research will focus on refining the Page curve, including the abovementioned aspects.

Appendix A

Taub-Nut space-time

This part is based on²⁴. The NUT solution is often quoted in the form

$$ds^2 = -f(r)(d\bar{t} - 2l \cos \theta d\phi)^2 + \frac{dr^2}{f(r)} + (r^2 + l^2)(d\theta^2 + \sin^2 \theta d\phi^2), \quad (\text{A.1})$$

where

$$f(r) = \frac{r^2 - 2mr - l^2}{r^2 + l^2}, \quad (\text{A.2})$$

and m and l are constants, of which l is known as the NUT parameter.

When $l = 0$ and $m \neq 0$, the metric reduces to the Schwarzschild solution in which m is the familiar parameter representing the mass of the source. However, when $l \neq 0$, the space-time has very different global properties to that of Schwarzschild

Because of the $l \cos \theta$ term in the metric (A.1), the space-time does not have a well-behaved axis at both $\theta = 0$ and $\theta = \pi$. However, it is possible to introduce a regular axis at $\theta = 0$ by applying the transformation $\bar{t} = t + 2l\phi$. This takes the line element (A.1) to

$$ds^2 = -f(r) \left(dt + 4l \sin^2 \frac{1}{2} \theta d\phi \right)^2 + \frac{dr^2}{f(r)} + (r^2 + l^2)(d\theta^2 + \sin^2 \theta d\phi^2). \quad (\text{A.3})$$

In terms of a natural tetrad with $\mathbf{k} = \frac{1}{f(r)}\partial_t + \partial_r$ and $\mathbf{l} = \frac{1}{2}\partial_t - \frac{f(r)}{2}\partial_r$, some of the spin coefficients are given by $\rho = -\frac{1}{r+il}$, $\kappa = \sigma = \lambda = \nu = 0$ and $\mu = -\frac{f(r)}{2(r+il)}$, and the only non-zero component of the Weyl tensor is

$$\Psi_2 = -\frac{m + il}{(r + il)^3}. \quad (\text{A.4})$$

From this it is clear that the space-time is associated with the gravitational field of a isolated massive object, and that both repeated principal null congruences are geodesic and shear-free but have non-zero expansion and twist. Moreover, the twist of each congruence is proportional to the NUT parameter l . This parameter may therefore initially be regarded as a twist parameter.

It may also be observed that this space-time is asymptotically flat in the sense that the Riemann tensor decays as r^{-3} as $r \rightarrow \pm\infty$. However, the metric clearly contains some kind of singularity along the half axis $\theta = \pi$. Thus the solution cannot be globally asymptotically flat.

Also, in contrast to the Schwarzschild solution, all components of the Riemann tensor are analytic functions of r over any range when $l \neq 0$: no scalar polynomial curvature singularity exists for any value of r . It is therefore natural for r to cover the full range $r \in (-\infty, \infty)$. However, a singularity of some kind clearly occurs whenever $f(r) = 0$. In fact, $f(r)$ given by (A.2) has two distinct roots with positive and negative values of r given by

$$r_{\pm} = m \pm \sqrt{m^2 + l^2}. \tag{A.5}$$

Appendix B

Derivation of the Bekenstein-Hawking entropy

In order to calculate the entropy a Schwarzschild black hole is considered in the calculations. The first law of thermodynamics for pressureless matter is given by⁹⁰

$$dE = T dS. \quad (\text{B.1})$$

Since the black holes have temperature, equal to the Hawking temperature, and energy, equal to their mass, the first law of thermodynamics can be written as

$$dM = T dS. \quad (\text{B.2})$$

Additionally, we know that the temperature is given by

$$T = \frac{1}{8\pi M}. \quad (\text{B.3})$$

Therefore, the expression (B.2) turns into

$$dS = 8\pi M dM. \quad (\text{B.4})$$

Finally, the entropy is given by

$$S = 4\pi M^2. \quad (\text{B.5})$$

Now, taking into account that the $r_h = 2M$, the are of the black hole is defined as follows

$$A = 16\pi M^2. \quad (\text{B.6})$$

Comparing, equations (B.5) and (B.6), it is possible to conclude that the entropy is given by

$$S = \frac{A}{4}, \quad (\text{B.7})$$

which is the well-known Bekenstein-Hawking entropy and it has been generalized for most of the metrics that describe a black hole.

Appendix C

Modeling the Time Evolution for the Kerr-Taub-Nut Black Hole Parameters

Considering the model 2.49 it is possible to have the following relations

$$-M^2 \frac{dM}{dt} = \alpha_1. \quad (\text{C.1})$$

$$-Ma_*^{-1} \frac{dM}{dt} = \alpha_2. \quad (\text{C.2})$$

$$-M^2 l_*^{-1} \frac{dL}{dt} = \alpha_3. \quad (\text{C.3})$$

Now using the expressions (3.32), (3.33), and (3.34) it is possible to obtain the following relations, setting $N = \sum_{\ell=0}^3 \sum_{m=0}^3 \frac{\gamma_{\ell m}(\omega)}{\exp(\omega/T_H) - 1} \frac{1}{2\pi}$; for mass:

$$-\frac{dM}{dt} = N \omega d\omega, \quad (\text{C.4})$$

for angular momentum:

$$-\frac{dJ}{dt} = N m d\omega, \quad (\text{C.5})$$

for nut charge:

$$-\frac{dL}{dt} = N n d\omega, \quad (\text{C.6})$$

where n is the fundamental nut charge defined in 3.3.2. Now, comparing the equations (C.4), (C.5), (C.6), (C.1), (C.2), and C.3 and making the change the change of variable $x = M\omega$, it is possible to get the expressions given by

$$-M^2 \frac{dM}{dt} = N x dx. \quad (\text{C.7})$$

$$-Ma_*^{-1} \frac{dM}{dt} = N m a_*^{-1} dx. \quad (\text{C.8})$$

$$-M^2 l_*^{-1} \frac{dL}{dt} = M N n l_*^{-1} dx. \quad (\text{C.9})$$

Looking Eq. (C.9), it is possible to see that the mass must be simplified suggesting that the model (2.49) does not work for the nut charge. Therefore,

$$-M l_*^{-1} \frac{dL}{dt} = N n l_*^{-1} dx. \quad (\text{C.10})$$

Now taking into account the right sides of expressions (C.7), (C.8), and (C.9) they must be equal to α_1 , α_2 , and α_3 . In the same way we have indirectly calculated the corresponding values as differential decays in 3.4. Therefore, it is possible to say that for the nut charge the time must be scaled as M^2 , instead of the time scaling for mass and angular momentum that is defined as M^3 . The models are expressed as follows

$$-M^2 \frac{dM}{dt} = \alpha_1. \quad (\text{C.11})$$

$$-M a_*^{-1} \frac{dM}{dt} = \alpha_2. \quad (\text{C.12})$$

$$-M l_*^{-1} \frac{dL}{dt} = \alpha_3. \quad (\text{C.13})$$

Appendix D

Mathematica code to calculate the entropy of Hawking radiation

```
1 (*Input the functions that describe the evolution parameters for a KTN black hole.*)
2 (*Function parameters*)
3 (*t: time, M0: initial mass, J0: initial angular momentum, L0: \
4 initial nut parameter,
5 a1:\[Alpha], a2:\[Alpha]2, a3:\[Alpha]3, as:Subscript[a, *], \
6 an:Subscript[l, *] *)
7
8 M[t_, M0_] := M0 (1 - t)^(1/3) (*for mass*)
9
10 J[t_, a1_, as_, a2_, M0_, J0_] := J0 - ((a2 as M0^2)/(2 a1))(1-(1-t)^(2/3)) (*for angular
11 momentum*)
12
13 L[t_, a1_, an_, a3_, M0_, L0_] := L0 - ((a3 an M0^2)/(2 a1))(1-(1-t)^(2/3)) (*for nut parameter
14 *)
15
16 (*The functions for angular momentum and nut parameter need to be reajusted
17 considering the decay time for each parameter.*)
18
19 JJ[t_, a1_, as_, a2_, M0_, J0_] :=
20 Piecewise[{{J[t, a1, as, a2, M0, J0],
21 0 <= t <= 1 - ((-2a1J0 + a2asM0^2)/(a2asM0^2))^(3/2)}, {0,
22 t > 1 - ((-2a1J0 + a2asM0^2)/(a2asM0^2))^(3/2)}}] (*for angular momentum*)
23
24 LL[t_, a1_, an_, a3_, M0_, L0_] :=
25 Piecewise[{{L[t, a1, an, a3, M0, L0],
26 0 <= t <= 1 - ((-2a1L0 + a3anM0^2)/(a3anM0^2))^(3/2)}, {0,
27 t > 1 - ((-2a1L0 + a3anM0^2)/(a3anM0^2))^(3/2)}}] (*for nut parameter*)
```

```
27 (*After that, the previous functions need to be replaced in the
28 Bekenstein-Hawking entropy for a KTN black hole given by Eq.(3.7).*)
29
30 S[t_, M0_, J0_, L0_, a1_, a2_, a3_, as_, an_] :=
31 2 Pi (M[t, M0]^2 + LL[t, a1, an, a3, M0, L0]^2 +
32      M[t, M0] Sqrt[
33          M[t, M0]^2 + LL[t, a1, an, a3, M0, L0]^2 -
34          JJ[t, a1, as, a2, M0, J0]^2/M[t, M0]^2])
35
36 (*Now, considering that Subscript[S, rad]= \[Beta] [(Subscript[S, \
37 BH](0)-Subscript[S, BH](t)].
38 Therefore, the entropy of the Hawking radiation is given by;*)
39
40 SR[t_] := \[Beta] (S[0, M0, J0, L0, a1, a2, a3, as, an] -
41      S[t, M0, J0, L0, a1, a2, a3, as, an])
```

Bibliography

- [1] Calmet, X. *Quantum aspects of black holes*; Springer, 2015; Vol. 178.
- [2] Auffinger, J. Primordial black hole constraints with Hawking radiation—a review. *Progress in Particle and Nuclear Physics* **2023**, 104040.
- [3] Almheiri, A.; Mahajan, R.; Maldacena, J.; Zhao, Y. The Page curve of Hawking radiation from semiclassical geometry. *Journal of High Energy Physics* **2020**, 2020, 1–24.
- [4] Page, D. N. Information in black hole radiation. *Physical review letters* **1993**, 71, 3743.
- [5] Mola Bertran, O. The black hole information paradox and holography. 2023.
- [6] Ryu, S.; Takayanagi, T. Holographic derivation of entanglement entropy from the anti–de sitter space/conformal field theory correspondence. *Physical review letters* **2006**, 96, 181602.
- [7] Penington, G. Entanglement wedge reconstruction and the information paradox. *Journal of High Energy Physics* **2020**, 2020, 1–84.
- [8] Miao, R.-X. Entanglement island and Page curve in wedge holography. *Journal of High Energy Physics* **2023**, 2023, 1–40.
- [9] Anand, A. Page curve and island in EGB gravity. *Nuclear Physics B* **2023**, 993, 116284.
- [10] Gan, W.-C.; Du, D.-H.; Shu, F.-W. Island and Page curve for one-sided asymptotically flat black hole. *Journal of High Energy Physics* **2022**, 2022, 1–30.
- [11] Awad, A. M. Higher dimensional Taub-nuts and Taub-bolts in Einstein–Maxwell gravity. *Classical and Quantum Gravity* **2006**, 23, 2849.
- [12] Ghasemi-Nodehi, M.; Chakraborty, C.; Yu, Q.; Lu, Y. Investigating the existence of gravitomagnetic monopole in M87. *The European Physical Journal C* **2021**, 81, 1–12.
- [13] Younsi, Z.; Grenzebach, A. Electromagnetic and observational signatures of the Kerr-Taub-NUT spacetime. 2018.

- [14] Haroon, S.; Jusufi, K.; Jamil, M. Shadow images of a rotating dyonic black hole with a global monopole surrounded by perfect fluid. *Universe* **2020**, *6*, 23.
- [15] Narzilloev, B.; Abdujabbarov, A.; Ahmedov, B.; Bambi, C. Kerr-Taub-NUT spacetime to explain the jet power and the radiative efficiency of astrophysical black holes. *Physical Review D* **2023**, *108*, 103013.
- [16] Page, D. N. Time dependence of Hawking radiation entropy. *Journal of Cosmology and Astroparticle Physics* **2013**, *2013*, 028.
- [17] Nian, J. Kerr black hole evaporation and Page curve. *arXiv preprint arXiv:1912.13474* **2019**,
- [18] Taub, A. H. Empty space-times admitting a three parameter group of motions. *Annals of Mathematics* **1951**, 472–490.
- [19] Wheeler, J. A. In *Essays in General Relativity*; Tipler, F. J., Ed.; Academic Press, 1980; pp 59–70.
- [20] Newman, E.; Tamburino, L.; Unti, T. Empty-space generalization of the Schwarzschild metric. *Journal of Mathematical Physics* **1963**, *4*, 915–923.
- [21] Foo, J.; Good, M. R.; Mann, R. B. Analog particle production model for general classes of taub-nut black holes. *Universe* **2021**, *7*, 350.
- [22] Grenzebach, A.; Perlick, V.; Lämmerzahl, C. Photon regions and shadows of Kerr-Newman-NUT black holes with a cosmological constant. *Physical Review D* **2014**, *89*, 124004.
- [23] Griffiths, J. B.; Podolský, J. *Exact space-times in Einstein's general relativity*; Cambridge University Press, 2009.
- [24] Podolský, J.; Vrátný, A. Accelerating NUT black holes. *Physical Review D* **2020**, *102*, 084024.
- [25] Hawking, S. W.; Ellis, G. F. *The large scale structure of space-time*; Cambridge university press, 2023.
- [26] Bonnor, W. B. A new interpretation of the NUT metric in general relativity. 1969.
- [27] Saha, M. The origin of mass in Neutrons and Protons. *Resonance* **1998**, *3*, 84–96.
- [28] Dirac, P. A. M. Quantised singularities in the electromagnetic field. *Proceedings of the Royal Society of London. Series A, Containing Papers of a Mathematical and Physical Character* **1931**, *133*, 60–72.
- [29] Plebanski, J. F.; Demianski, M. Rotating, charged, and uniformly accelerating mass in general relativity. *Annals of Physics* **1976**, *98*, 98–127.
- [30] Yang, S.-J.; Chen, J.; Wan, J.-J.; Wei, S.-W.; Liu, Y.-X. Weak cosmic censorship conjecture for a Kerr-Taub-NUT black hole with a test scalar field and particle. *Physical Review D* **2020**, *101*.

- [31] Abdujabbarov, A. A.; Ahmedov, B. J.; Kagramanova, V. G. Particle motion and electromagnetic fields of rotating compact gravitating objects with gravitomagnetic charge. *General Relativity and Gravitation* **2008**, *40*, 2515–2532.
- [32] Narzilloev, B.; Abdujabbarov, A.; Ahmedov, B.; Bambi, C. Kerr-Taub-NUT spacetime to explain the jet power and the radiative efficiency of astrophysical black holes. *Phys. Rev. D* **2023**, *108*, 103013.
- [33] Mukhopadhyay, B.; Dadhich, N. Scalar and spinor perturbation to the Kerr–NUT spacetime. *Classical and Quantum Gravity* **2004**, *21*, 3621.
- [34] Abdujabbarov, A.; Ahmedov, B.; Shaymatov, S.; Rakhmatov, A. Penrose process in Kerr-Taub-NUT spacetime. *Astrophysics and Space Science* **2011**, *334*, 237–241.
- [35] Miller, J. Global analysis of the Kerr-Taub-NUT metric. *Journal of Mathematical Physics* **1973**, *14*, 486–494.
- [36] Hackmann, E.; Lämmerzahl, C. Observables for bound orbital motion in axially symmetric space-times. *Physical Review D* **2012**, *85*, 044049.
- [37] Ferrari, V.; Gualtieri, L.; Pani, P. *General relativity and its applications: black holes, compact stars and gravitational waves*; CRC press, 2020.
- [38] Carroll, S. M. *Spacetime and geometry*; Cambridge University Press, 2019.
- [39] Chakraborty, C.; Bhattacharyya, S. Circular orbits in Kerr-Taub-NUT spacetime and their implications for accreting black holes and naked singularities. *Journal of Cosmology and Astroparticle Physics* **2019**, *2019*, 034–034.
- [40] Mukherjee, S.; Chakraborty, S.; Dadhich, N. On some novel features of the Kerr–Newman-NUT spacetime. *The European Physical Journal C* **2019**, *79*, 1–24.
- [41] Lan, C.; Yang, H.; Guo, Y.; Miao, Y.-G. Regular black holes: A short topic review. *International Journal of Theoretical Physics* **2023**, *62*, 202.
- [42] Wald, R. M. *Quantum field theory in curved spacetime and black hole thermodynamics*; University of Chicago press, 1994.
- [43] Konoplya, R. A.; Stuchlík, Z.; Zhidenko, A. Axisymmetric black holes allowing for separation of variables in the Klein-Gordon and Hamilton-Jacobi equations. *Phys. Rev. D* **2018**, *97*, 084044.
- [44] Teukolsky, S. A. Rotating Black Holes: Separable Wave Equations for Gravitational and Electromagnetic Perturbations. *Phys. Rev. Lett.* **1972**, *29*, 1114–1118.
- [45] Teukolsky, S. A. Perturbations of a Rotating Black Hole. I. Fundamental Equations for Gravitational, Electromagnetic, and Neutrino-Field Perturbations. **1973**, *185*, 635–648.

- [46] Don, P. Particle emission rates from a black hole: Massless particles from an uncharged, non-rotating hole. *Physical Review D* **13**.
- [47] Jian, Y.; Zheng, Z.; Gui-Hua, T.; Wen-Biao, L. Tortoise coordinates and hawking radiation in a dynamical spherically symmetric spacetime. *Chinese Physics Letters* **2009**, *26*, 120401.
- [48] Ganjali, M. On Effective Potential in Tortoise Coordinate. *International Journal of Theoretical Physics* **2012**, *51*, 2380–2391.
- [49] Pitalua Pantoja, J. L. Evaporación de un agujero negro de Schwarzschild y potenciales efectivos. Ph.D. thesis, Universidad Nacional de Colombia.
- [50] Hawking, S. W. Particle creation by black holes. *Communications in mathematical physics* **1975**, *43*, 199–220.
- [51] Almheiri, A.; Hartman, T.; Maldacena, J.; Shaghoulian, E.; Tajdini, A. The entropy of Hawking radiation. *Reviews of Modern Physics* **2021**, *93*, 035002.
- [52] Övgün, A.; Jusufi, K. Quasinormal modes and greybody factors of $f(R)$ gravity minimally coupled to a cloud of strings in 2+1 dimensions. *Annals of Physics* **2018**, *395*, 138–151.
- [53] Schutz, B. *Gravity from the ground up: An introductory guide to gravity and general relativity*; Cambridge university press, 2003.
- [54] Bekenstein, J. D. Black Holes and Entropy. *Phys. Rev. D* **1973**, *7*, 2333–2346.
- [55] Harlow, D. Jerusalem lectures on black holes and quantum information. *Reviews of Modern Physics* **2016**, *88*, 015002.
- [56] Rahman, I. A. On the Black Hole Information Paradox and the Page Curve.
- [57] Escobedo, J. Greybody factors: Hawking radiation in disguise. Ph.D. thesis, Masters Thesis, University of Amsterdam, 2008.
- [58] Maldacena, J.; Strominger, A. Black hole greybody factors and D-brane spectroscopy. *Physical Review D* **1997**, *55*, 861–870.
- [59] Gogoi, D. J.; Övgün, A.; Demir, D. Quasinormal modes and greybody factors of symmergent black hole. *Physics of the Dark Universe* **2023**, *42*, 101314.
- [60] Kanti, P.; March-Russell, J. Calculable corrections to brane black hole decay: The scalar case. *Phys. Rev. D* **2002**, *66*, 024023.
- [61] Panotopoulos, G.; Rincón, Greybody factors for a minimally coupled scalar field in a three-dimensional Einstein-power-Maxwell black hole background. *Physical Review D* **2018**, *97*.

- [62] Pantig, R. C.; Mastrototaro, L.; Lambiase, G.; Övgün, A. Shadow, lensing, quasinormal modes, greybody bounds and neutrino propagation by dyonic ModMax black holes. *The European Physical Journal C* **2022**, *82*.
- [63] Unruh, W. Absorption cross section of small black holes. *Physical Review D* **1976**, *14*, 3251.
- [64] Al-Badawi, A.; Sakallı, İ.; Kanzi, S. Solution of Dirac equation and greybody radiation around a regular Bardeen black hole surrounded by quintessence. *Annals of Physics* **2020**, *412*, 168026.
- [65] Boonserm, P.; Visser, M. Bounding the greybody factors for Schwarzschild black holes. *Physical Review D* **2008**, *78*, 101502.
- [66] Kanti, P.; March-Russell, J. Calculable corrections to brane black hole decay: The scalar case. *Physical Review D* **2002**, *66*, 024023.
- [67] Sharif, M.; Ama-Tul-Mughani, Q. Greybody factor for a rotating Bardeen black hole. *The European Physical Journal Plus* **2019**, *134*, 616.
- [68] Sharif, M.; Shaikat, S. Greybody factor for a rotating Bardeen black hole by perfect fluid dark matter. *Annals of Physics* **2022**, *436*, 168673.
- [69] Creek, S.; Efthimiou, O.; Kanti, P.; Tamvakis, K. Scalar emission in the bulk in a rotating black hole background. *Physics Letters B* **2007**, *656*, 102–111.
- [70] Sampaio, M. O. Distributions of charged massive scalars and fermions from evaporating higher-dimensional black holes. *Journal of High Energy Physics* **2010**, *2010*, 1–21.
- [71] Gautason, F. F.; Schneiderbauer, L.; Sybesma, W.; Thorlacius, L. Page curve for an evaporating black hole. *Journal of High Energy Physics* **2020**, *2020*, 1–23.
- [72] Nam, C. H. Entanglement entropy and Page curve of black holes with island in massive gravity. *The European Physical Journal C* **2022**, *82*, 381.
- [73] Karpatitis, A. Evaporating Black Holes and the Page Curve. Ph.D. thesis, University of Cyprus, 2021.
- [74] Blundell, S. J.; Blundell, K. M. *Concepts in thermal physics*; Oup Oxford, 2010.
- [75] Susskind, L.; Lindesay, J. *Introduction To Black Holes, Information And The String Theory Revolution, An: The Holographic Universe*; World Scientific, 2004.
- [76] Page, D. N. Particle emission rates from a black hole. II. Massless particles from a rotating hole. *Physical Review D* **1976**, *14*, 3260.
- [77] Taylor, B. E.; Chambers, C. M.; Hiscock, W. A. Evaporation of a Kerr black hole by emission of scalar and higher spin particles. *Physical Review D* **1998**, *58*.

- [78] Siahhaan, H. M. Magnetized Kerr-Taub-NUT spacetime and Kerr/CFT correspondence. *Physics Letters B* **2021**, *820*, 136568.
- [79] Hartle, J.; Wilkins, D. Analytic properties of the Teukolsky equation. *Communications in Mathematical Physics* **1974**, *38*, 47–63.
- [80] Seidel, E. A comment on the eigenvalues of spin-weighted spheroidal functions. *Classical and Quantum Gravity* **1989**, *6*, 1057.
- [81] Panotopoulos, G.; Rincón, Á. Greybody factors for a minimally coupled scalar field in a three-dimensional Einstein-power-Maxwell black hole background. *Physical Review D* **2018**, *97*, 085014.
- [82] Leite, L. C.; Benone, C. L.; Crispino, L. C. On-axis scattering of scalar fields by charged rotating black holes. *Physics Letters B* **2019**, *795*, 496–501.
- [83] Hochberg, D.; Kephart, T. W.; York Jr, J. W. Effective potential of a black hole in thermal equilibrium with quantum fields. *Physical Review D* **1994**, *49*, 5257.
- [84] Teixeira da Costa, R. Mode Stability for the Teukolsky Equation on Extremal and Subextremal Kerr Spacetimes. *Communications in Mathematical Physics* **2020**, *378*, 705–781.
- [85] Sun, Q.; Li, Q.; Zhang, Y.; Li, Q.-Q. Quasinormal modes, Hawking radiation and absorption of the massless scalar field for Bardeen black hole surrounded by perfect fluid dark matter. *arXiv preprint arXiv:2302.10758* **2023**,
- [86] Kanti, P. Black holes in theories with large extra dimensions: a review. *International journal of modern physics A* **2004**, *19*, 4899–4951.
- [87] Kokkotas, K.; Konoplya, R.; Zhidenko, A. Quasinormal modes, scattering, and Hawking radiation of Kerr-Newman black holes in a magnetic field. *Physical Review D* **2011**, *83*, 024031.
- [88] Brito, R.; Cardoso, V.; Pani, P. *Superradiance: Energy Extraction, Black-Hole Bombs and Implications for Astrophysics and Particle Physics*; Springer International Publishing, 2015.
- [89] Page, D. N. Hawking radiation and black hole thermodynamics. *New Journal of Physics* **2005**, *7*, 203.
- [90] Greiner, W.; Neise, L.; Stöcker, H. *Thermodynamics and statistical mechanics*; Springer Science & Business Media, 2012.